GEOGRAPHICA AUGUSTANA

Jacobeit / Philipp / Rathmann / Walther

E M U L A T E

European and North Atlantic
daily to **mult**idecadal clim**ate** variability

Objectives and Results of the
German Contribution to the European
Climate Research Project EMULATE

01

4

010 067 stitut für Geographie UNIVERSITÄT AUGSBURG **Band 7**

Jucundus Jacobeit, Andreas Philipp,
Joachim Rathmann, Alexander Walther

European and North Atlantic Daily to
Multidecadal
Climate Variability

General Overview and Final Reports
for the German contribution to the
European Climate Research Project EMULATE

Jucundus Jacobeit, Andreas Philipp, Joachim Rathmann, Alexander Walther

European and North Atlantic Daily to Multidecadal

Climate Variability

General Overview and Final Reports

for the German contribution to the

European Climate Research Project EMULATE

Augsburg 2009

List of Figures

List of Tables

1   General Overview for the entire project

Empirical studies of the influence of atmospheric circulation on surface climate are limited by data availability. The Project Summary from the official EMULATE website addresses some important aspects in this context: since the instrumental database is short, it is often difficult to discern whether relationships are stationary or subtle changes are occurring. Europe has the longest instrumental climate records world-wide, as the first instruments were developed there from the mid-17- century onwards. Although earlier research projects have highlighted some of these records, others wait to be digitised and homogenised. Therefore, digital availability and homogeneity issues are still the principal constraints for long-term analyses of large-scale circulation patterns and their influence on European surface climate variations.

Many analyses do not start before the mid-20th century (reanalyses period), whereas the EU-project ADVICE (Annual to Decadal Variability in Climate in Europe) was a first step to extend the objective reconstruction of sea level pressure (SLP) fields and the statistical analysis of circulation dynamics further back in time until the end of the 18th century (see Jones et al. 1999; Jacobeit et al. 1998; Beck 2000; Jacobeit et al. 2001). These pressure fields, however, have only a monthly resolution, similar as further reconstructions (Luterbacher et al. 2002) going back to the mid-17th century or – on a seasonal scale – even to the year 1500 AD. The focus of EMULATE has now been to extend analyses on a daily scale further back in time, and this seems to be feasible at present until the mid-19th century.

The European research project EMULATE was funded by the European Commission for the 40-month period from November 2002 until February 2006. This project was established in the context of the Fifth Framework Research Programme "Energy, Environment and Sustainable Development", Key Action "Global Change, Climate and Biodiversity", co-ordinated by Prof. Phil Jones from the Climatic Research Unit (CRU) at the University of East Anglia in Norwich (UK). The acronym EMULATE is derived from the title "European and North Atlantic daily to multidecadal climate variability". The following partners were involved in EMULATE (with their acronyms used below added in parentheses):

1. University of East Anglia, UK (UEA)
2. Hadley Centre of the Meteorological Office, UK (MetO)
3. University of Würzburg/Augsburg, Germany (UWUERZ/UAUGS)*
4. CEA's Laboratoire des Sciences du Climat et de l'Environnement, France (CEA)
5. University Rovira i Virgili, Tarragona, Spain (URV)
6. University of Bern, Switzerland (UBERN)
7. Stockholm University, Sweden (SU)
8. University of Gothenburg, Sweden (UGOT)

*the German partner has moved from Würzburg to Augsburg during the funding period of EMULATE.

Main scientists of the consortium have been for

UEA: Phil Jones, David Lister,
MetO: Chris Folland, David Parker, Adam Scaife, Jeff Knight, Rob Allan, Tara Ansell,
UAUGS: Jucundus Jacobeit, Andreas Philipp, Joachim Rathmann,
CEA: Pascal Yiou, Nicolas Fauchereau,
URV: Manola Brunet-India,

UBERN: Heinz Wanner, Juerg Luterbacher, Paul Della-Marta,
SU: Anders Moberg,
UGOT: Deliang Chen, Alexander Walther*

*at UWUERZ during the first part of the project.

Primary objective of EMULATE has been the analysis of long-term climate variability on a daily time-scale. According to the Project Summary from the official EMULATE website the following scientific achievements can be summarized: EMULATE has extended North-Atlantic-European analyses back to the mid-19th century, providing more than 150 years of gridded daily mean sea-level pressure (MSLP) data for the extratropical North Atlantic and European region. The database has been assessed for quality and standard errors quantified for each time step and grid-point location. The data set has been used to develop daily and longer time-scale characteristic atmospheric circulation patterns over the study region for each overlapping two-month season (JF, FM, MA, AM, MJ, JJ, JA, AS, SO, ON, ND, DJ)[1] and each traditional three-month season (DJF, MAM, JJA, SON)[1] of the year. Variations and trends in these circulation patterns and associated temperature and precipitation patterns have been related to those evident in large-scale sea surface temperatures (SSTs) and other possible oceanic fluctuations including those of the thermohaline circulation, with the aid of atmosphere-only and coupled atmosphere-ocean models. Variations in the incidence of extremes of temperature and precipitation (including drought) across Europe have been related to variations and trends in the atmospheric circulation patterns on daily to multi-decadal time scales and to SSTs and possible anthropogenic factors. With the new datasets and patterns, relationships have been investigated for much longer periods than so far available.

---

[1] JF: January, February – FM: February, March - ... - DJF: December, January, February - ...

2   Scientific Objectives

The study period for the whole project on North-Atlantic-European climate variability is 1850-2003. It is assumed that the effects of human activities on the climate system became significant not before the turn to the 20th century. Thus, with a timeframe starting in 1850, there are about 50 years without much man-made impact on climate. The extended daily MSLP record generated as the first outcome of EMULATE has enabled a more reliable assessment of the relative importance of anthropogenic factors in circulation and climate dynamics. Relationships (and their variability) which have been found based on observational data, have additionally been compared with results from the Hadley Centre atmosphere-only and coupled climate models.

The research of the entire project (not only the German part) has been focussed on four main objectives (these descriptions largely follow the official EMULATE website with respect to "Scientific Objectives"):

Objective 1: Create daily gridded MSLP fields from 1850

This fundamental aim of EMULATE refers to the North-Atlantic-European area (25°N – 70°N, 70°W – 50°E) covered by a regular grid with a 5° by 5° resolution.

EMULATE has used already available gridded daily fields for Europe after 1881 adjusted to be consistent with recently produced homogeneous monthly pressure fields. These gridded fields are available from the two UK partners. The data base has subsequently been extended by digitising daily station pressure data for the 1850-1880 period, particularly including peripherical regions like Eastern Europe and the Eastern Mediterranean area.

Exploratory studies have indicated that no more than about 40 additional daily MSLP series for 1850-1880 have been required, as many long-term daily series are already available from earlier EU and national research projects. Over the ocean areas, EMULATE has used the new blend of the Met Office marine data bank with the recently enhanced International Comprehensive Ocean Atmosphere Data Set (now named I-COADS) and recently digitized marine data from Norway and other sources. In particular the marine pressure data is a considerable enhancement compared to data sets previously available. In addition, daily station data for several eastern North American locations (from Canadian and US colleagues) have been included into the large-scale analysis.

Analyses of climate variability tend to be more effective if they use data interpolated to a regular grid. This is because interpolation enables both spatially and temporally complete and more internally consistent datasets to be produced which are more amenable to many of the complex multivariate analysis techniques now available. All presently available interpolation methods are based on correlation or covariance matrices and least-squares theory. Most produce similar results, particularly when the relationships between predictors and predictands are strong.

EMULATE has intercompared several methods (e.g. simple linear interpolation and more complex optimal interpolation methods which include principal components of the basic data) to determine the best one and the impacts of each method on resulting products. Errors of estimation have been calculated for the best method.

Objective 2: Derive a set of characteristic atmospheric circulation patterns, and study their variations and trends for each season

EMULATE has considered several techniques, including various types of cluster analysis, principal component analysis (PCA) and non-linear PCA (NLPCA), to derive characteristic atmospheric circulation patterns. The surface climate of Europe is strongly influenced by many circulation factors. Of these, the North Atlantic Oscillation (NAO) is best known, but other patterns are often equally important. For example, the recent heavy precipitation and resultant flooding in north-western Europe (April 2000-April 2001 and especially the autumn months in 2000) was unrelated to the NAO and resulted from persistent blocking over western and northern Europe. The heavy floodings in Central Europe during summertime in 1997 and 2002 have been linked to particular cyclone tracks (variants of van Bebber's Vb pattern) in connection with further dynamical conditions favouring extreme precipitation. Among the different techniques for an overall pattern classification, advanced approaches like simulated annealing clustering have proved to be especially successful.

Objective 3: Relate variations and trends in atmospheric circulation and associated surface climate variability over Europe to sea surface temperature patterns, particularly from the North Atlantic

Winter temperatures and precipitation amounts in Europe are known to be quite strongly influenced by the NAO and may also be affected by other circulation and sea surface temperature (SST) patterns. Summer precipitation totals in Europe are less influenced by the NAO, but show marked multidecadal variability and are related to global-scale SST and atmospheric circulation variability. The nature and importance of multidecadal relationships between both SST and the atmospheric circulation and precipitation and temperature has been investigated with the help of the extended data sets which have been created by this project (see Objective 1). The long-term instrumental records, together with climate model data, have also been used to assess the importance of external climate forcing factors (including anthropogenic ones) to determine whether influences are changing.

Relationships also exist between regional-scale SSTs and atmospheric circulation patterns for the North Atlantic and the spatial and temporal scale of drought patterns in Europe. The temporal behaviour of such relationships has been investigated, with special emphasis on studying possible anthropogenic influences. The Mediterranean region is particularly sensitive to droughts and any increased ability to predict future droughts would be of great benefit to these countries.

Objective 4: Relate variations and trends in atmospheric circulation patterns to prominent extremes in temperature and precipitation

There is increasing concern that extreme climate (including weather time-scale) events which have major impacts on society and ecosystems, may be changing in frequency and character as a result of human impacts on climate. EMULATE has defined these extreme events based on long-term daily temperature and precipitation time series across Europe and has started to determine the importance of atmospheric circulation changes. EMULATE has also tried to assess the part that human impacts (directly or indirectly) may have played in changes in the frequency and severity of extreme events, enabled by using results from Hadley Centre climate model runs with both all forcings and only natural ones.

EMULATE has been divided into five **workpackages** (WP 1 to WP 5, see Fig. 1). The issues discussed in this volume are mainly related to WP 2, WP 3 and WP 4. The entire set of WPs includes the following brief titles (WP leaders added in parentheses):

14

Workpackages:

WP 1: Create daily gridded MSLP fields from 1850 (led by Phil Jones)
WP 2: Derive a set of characteristic atmospheric circulation patterns, and study their variations and trends for each season (led by Jucundus Jacobeit)
WP 3: Relate variations and trends in atmospheric circulation and associated surface climate variability over Europe to sea surface temperature patterns, particularly from the North Atlantic (led by Chris Folland)
WP 4: Relate variations and trends in atmospheric circulation patterns to prominent extremes in temperature and precipitation (led by Anders Moberg)
WP 5: Dissemination and Exploitation of Results (led by Phil Jones)
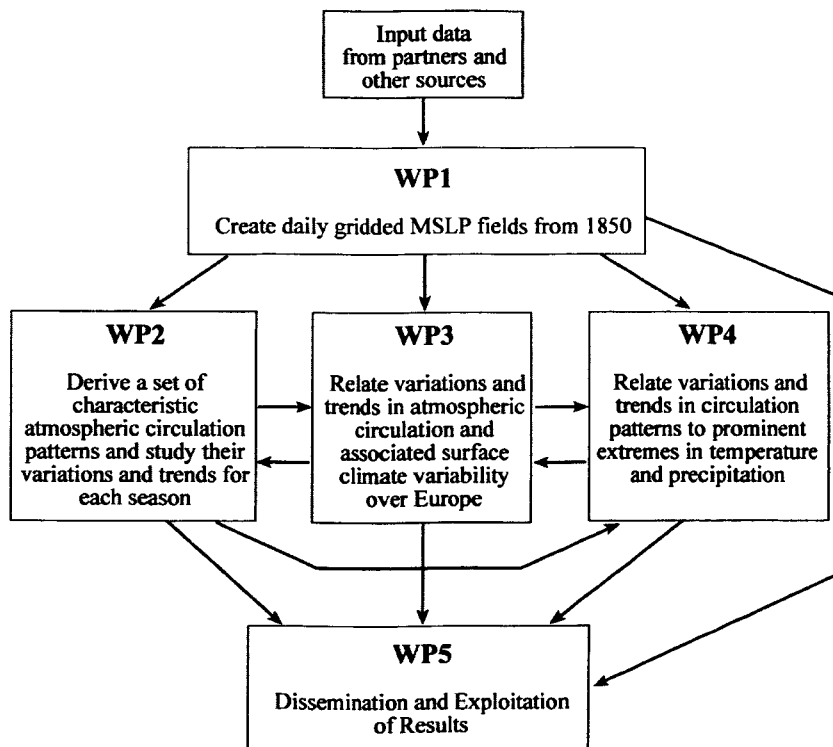
Fig. 1: The work-package structure of EMULATE (taken from the official website).

The German working group has focussed on WP 2 and WP 4, but also contributed to WP 1 and WP 3. Project output in terms of Deliverables (datasets and/or reports) is linked to public websites. The following Deliverables of EMULATE arise from the different workpackages of Fig. 1:

Deliverables with current number and brief deliverable title:

- D1: Project website
- D2: Daily pressure data for additional 40 stations for 1850-1880
- D3: Daily gridded fields of MSLP over the extratropical North Atlantic and Europe
- D4: Daily fields of MSLP made available to wider community via the website
- D5: Fields defining leading atmospheric circulation patterns for 2-month and 3-month seasons

- D6: Database of daily pattern amplitudes since 1850
- D7: Assessment of the variability of the observed North Atlantic and European atmospheric circulation for the last 150 years in relation to SST patterns
- D8: Gridded database of drought index for Europe
- D9: Time series of selected 'extremes' indices, based on temperature and precipitation, of value to society at a set of homogeneous daily stations covering Europe
- D10: Assessments of trends in pattern amplitudes and in the incidence of amplitude extremes
- D11: Assessment of the time-varying influence of SST and atmospheric circulation on European surface temperature and precipitation patterns
- D12: Results of model experiments to determine if the observed relationships in D7 and D11 are reproduced or can be better resolved using the longer time scales of the coupled model experiments, and an initial study of mechanisms and potential predictability.
- D13: Assessment of the relative influence of external forcing factors (natural and human) and internal variability and their seasonal differences
- D14: Assessments of changes in such extremes since the late nineteenth century
- D15: Assessments of the influence of atmospheric circulation variations on the incidence of extremes
- D16: Assessment of the likelihood of any anthropogenic influence on extremes
- D17: Final technical report to EU

The German working group has contributed to D2, D5, D6, D7, D9, D10, D11, D14 and D15.

Additional information on this project is available via the website of the co-ordinating institution, the Climatic Research Unit (CRU) at the University of East Anglia in Norwich, UK (http://www.cru.uea.ac.uk/projects/emulate). Concerning the German contributions results are also available from http://geo21/emulate.

The following chapters highlight these German contributions to EMULATE: Section 3 describes the compilation of a database referring to daily European station time series of temperature and precipitation including some selected trend matrices; furthermore, 64 different extremes indices are described. Sections 4, 5 and 6 summarize the German contributions to Workpackages 2, 3 and 4, respectively, largely corresponding to different parts of the final reports to the European Commission. Section 7 focusses on main results and progress achieved by the German working group during EMULATE.

3 Daily temperature and precipitation data of Europe

3.1 Basic informations

The set of stations used for analyses is related to the dimensions of the EMULATE MSLP field (25°N to 70°N and 70°W to 50°E), only the easterly limit has been stretched slightly. This seemed to be useful in view of the availability of Russian daily station data going back to about 1890.

Working steps and general aims of this preparatory part of EMULATE can be summarized as follows:

- compile daily temperature and precipitation data of (mainly) European stations and convert all data sets into a common format
- compile meta data as far as possible
- check the quality of data and correct obvious errors
- provide the new data base with an appropriate documentation
- compile trend matrices for regional climatic time series based on these data
- define particular extremes indices for temperature and precipitation
- compute time series of the extremes indices
- scan these extremes time series for linear trends
- map the spatial distributions of index values

EMULATE has developed a data base, for 230 European stations, with daily temperature and precipitation records going back at least to 1900. There were three main sources; (i) public available data bases, (ii) digitization of original data and (iii) personal contacts with data holders in many countries. Beside national weather services, the European Climate Assessment & Dataset (ECA&D) provides a substantial database containing daily station datasets in Europe. More than 20 stations have been added to the ECA&D data to create a new database containing European station data with a daily resolution. This database has subsequently been used for further analyses within EMULATE. According to the aims of EMULATE to study "daily to multidecadal climate variability", both short-term (daily to annual) as well as long-term (decadal to multidecadal) variability with particular reference to extreme events should be analysed. Therefore, a set of appropriate extremes indices must have been defined (see section 3.3). The spatial distribution of corresponding index values, however, has only been represented for selected examples without performing a detailed analysis of spatial patterns (being a separate task in the future).

The periods covered by data are quite different for the individual stations. Only 19 of them provided observations before 1850, the majority of series has starting dates between 1850 and 1890.

Four climatic variables have been focussed as basic data:
- daily minimum temperature (Tmin)
- daily maximum temperature (Tmax)
- daily mean temperature (Tmean)
- daily precipitation amount (prec)

Usually Tmin and Tmax are available at the same time (even if the periods covered by the two variables are identical for only 50 out of 90 stations). The presence of values for Tmin/Tmax does not necessarily mean, however, that there are values for Tmean as well and vice versa. Responsible for this are the different methods of measuring daily minimum/maximum temperatures and of

calculating daily mean temperatures. For the measurement of Tmin and Tmax, special extreme thermometers are commonly used. Daily means are often computed from hourly observations at particular times. One traditional method for the calculation of Tmean is the so-called "Mannheimer Stunden" formula:

$$T_{mean} = \frac{T_7 + T_{14} + 2 * T_{21}}{4}$$

Temperatures measured at 7:00 (7 am), 14:00 (2 pm) and 21:00 (9 pm) have to be used with a particular weighting. This method was established in 1790 by the Societas Meteorologica Palatina in Mannheim (Germany) and is mainly used for mid-latitude stations. Another approach is to compute the unweighted mean of temperatures observed at 1 am, 7 am, 1 pm and 7 pm. In recent times, of course, computer-aided observations with automatic thermometers allow to compute daily mean temperatures based on considerably more than 4 hourly observations.

Records with hourly observations are available at least for some stations. For example, the series of Helsinki (Finland/60.32°N/24.97°E) includes the hourly observations that are needed for the "Mannheimer Stunden" formula. For two of the Swiss stations (Bern (46.93°N/7.42°E); Grand-St-Bernard (45.87°N/7.17°E)) T_{mean} has been calculated using the slightly different hourly values being available (T7, T13, T19 or T21). Such kinds of procedure have to be documented and considered when using the datasets. For one station (Falun, Sweden/60.62°N/15.67°E) a specially adjusted formula could be used. An example of probably unsuitable temperature data – at least at present – are the hourly measurements for Stykkisholmur (Iceland/65.08°N/22.73°W) where the hours of observations have been changed several times during the whole period of measurements.

For some other stations, T_{mean} has been calculated as mean value of T_{min} and T_{max}:

$$T_{mean} = \frac{T_{min} + T_{max}}{2}$$

This method is obviously not the best one (although widely used). In the available time series of some stations it was found that the bulk of T_{mean} values correspond to mean values of T_{min} and T_{max} (e.g. for Brussels (50.90°N/4.53°E) around 50%, for Milano (45.50°N/9.20°E) around 70%).

The stations in Iceland (5) and Greenland (2) are the only data sources for the northwestern part of the study area. Unfortunately, the Icelandic dataset does not include any temperature data and suffers from a rather low quality. The percentages of missing values per year and station reach at least 20%.

Initially, observations with any of the four basic variables (T_{min}, T_{mean}, T_{max}, Prec) available before 1890 and located in the area of interest have been collected for EMULATE. It has turned out, however, that the available stations are distributed very unevenly. The station density is highest in some central parts of Europe (Netherlands, Denmark, Germany, Austria, Switzerland, Northern Italy) whereas for other regions no stations are available at all. The patterns of station density change if we distinguish between temperature and precipitation time series. To improve station density for some parts of the area of interest, the requirements have been abated, i.e. later starting years have been accepted for these areas. In this way further stations in Russia, Spain, Greenland and Austria have been included into the dataset (11 stations starting between 1891 and 1895; 2 stations starting in 1901). For such later starting years additional stations would also be available for other regions (especially in Germany), but this would perpetuate an uneven station density for Europe in general. Note that there is a sufficient number of stations allowing

to extend the study period back in time, the longest record (Padova 45.40°N/11.90°E) even going back to 1725.
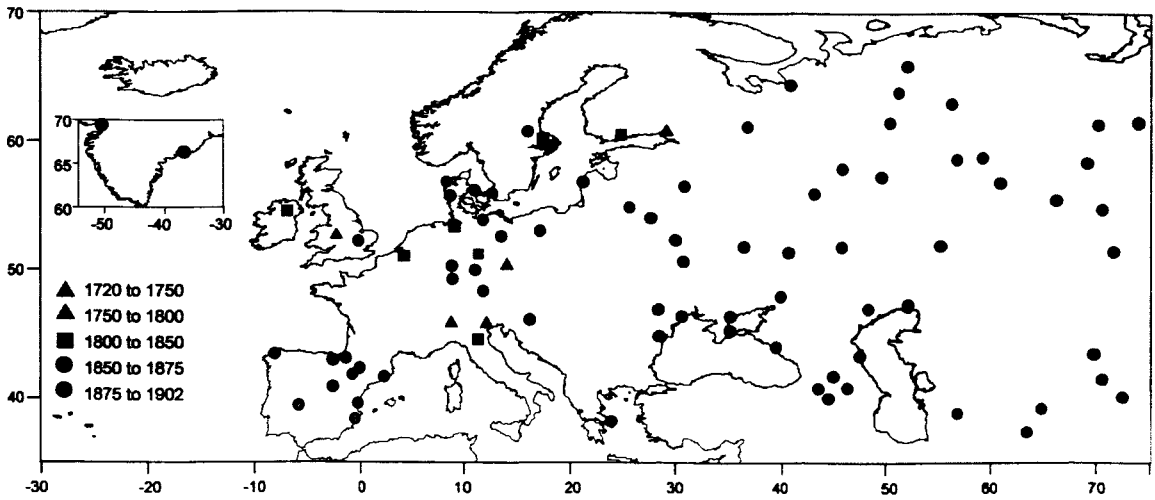
Fig. 2: Classified starting years of the available T_{min}/T_{max} time series (90 stations).
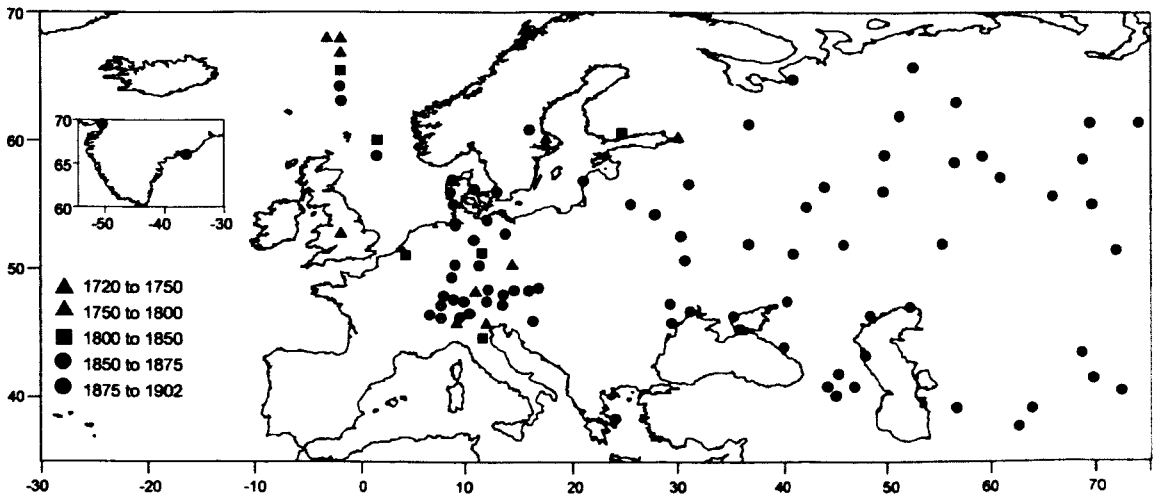
Fig. 3: Classified starting years of the available (received and computed) T_{mean} time series (95 stations).

There are 90 stations providing T_{min}/T_{max} and 95 stations providing T_{mean} time series (see Figs. 2 and 3). Some central parts of Europe (Southern Germany, Austria, Switzerland, Northern Italy) provide a satisfactory number of temperature observations, whereas in northern Europe (Sweden, Norway, Finland, Iceland) and in parts of southern Europe (Southern Italy, Greece, Turkey) only a few stations or no stations at all are available. Interpolation methods could help to combat the problems of irregular station density, but this has been beyond the scope of EMULATE.

The locations of stations with precipitation data are shown in Fig. 4. Compared to the temperature stations, there is a much larger number of stations for precipitation (142). Nevertheless, it is well-

known that precipitation characteristics may change on very small spatial scales. Interpolations would have to be based on appropriate numbers of locations providing precipitation data. In particular, topographical conditions are important factors modifying rainfall characteristics on small spatial scales. Indeed, topographical variance within the study area is rather high, especially in high mountain areas (station with highest elevation: Sonnblick (Austria), 3106 m asl). This defines the requirement of further enhancing the density of rainfall stations as far as possible.
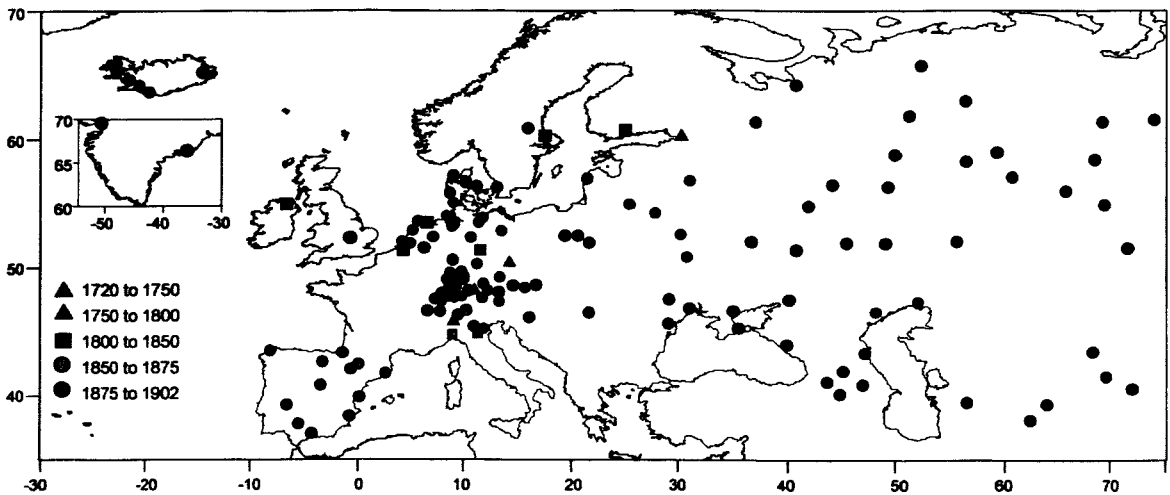
Fig. 4: Classified starting years of the available precipitation time series (142 stations).

3.2   Quality of Datasets

Several procedures for checking data quality have been applied to series for Germany and Russia by the data providers. Values have been flagged as 'OK', 'suspect' or 'not available'. These pre-tests have been used as a basis for further tests checking the consistency of the data. The following issues have mainly been focussed:

- correct relations between temperature values ($T_{min} < T_{mean} < T_{max}$)
- homogeneity of each station dataset
- quota of missing values

For scientific research unchecked datasets can not be very useful. In particular, if extreme events are to be analysed, a sufficient reliability of the original data is required. Complete meta data are vitally important for each station. On the basis of such data, it is often possible to find irregularities within the datasets. Despite the fundamental importance of homogeneous data for further analyses, it has been far beyond the scope of EMULATE to process the whole spectrum of sophisticated quality checks and homogenisation procedures, respectively.

3.3   Trend matrices for regional climatic time series

Trend matrices for the EMULATE period 1850-2003 have been calculated for moving 20-day periods within the 3-month seasons DJF, MAM, JJA, SON and the 2-month seasons JF, MA, MJ, JA, SO, ND both for daily mean temperature and daily precipitation. Figs. 5-8 include the 3-month seasons'

results based on station data for two European regions ("Germany" comprising 13 stations for temperature and 33 stations for precipitation (additionally including Prague), "Greater Alpine Region" with 11 stations for temperature and 13 stations for precipitation). The determination of these regions (and of four other ones within the EMULATE domain) is described in more detail by Moberg et al. (2006). Trends have been calculated for all periods greater or equal than 20 years, statistical significance has been determined by the non-parametric Mann-Kendall trend test. Obviously there are some inhomogenities e.g. for temperature during winter and autumn around 1940 or 1920, and for precipitation in the Greater Alpine Region during summer around 1870.

Results for temperature may be summarized as follows: Trends in the transitional seasons are generally lower and often insignificant compared to winter and summer. The trend patterns are more distinct in the Germany Region than in the Greater Alpine Region. During winter, there are two major cooling periods (in the last third of the 19th century and between 1915 and 1940) and two major warming periods (at the beginning and at the end of the 20th century). During summer, there is a distinct cooling at the beginning of the study period, a slight warming around the second cooling in winter, another cooling between 1940 and 1960, and a recent warming less striking than in winter.

Results for precipitation may be summarized as follows: For Germany there are distinct rising trends from the beginning of the study period which are maintained for end-years throughout the whole study period, especially pronounced during winter. In the Greater Alpine Region this phenomenon, much less intensive, is only observed during winter (but with decreasing trends until the early 20th century). During the first half of the 20th century there are some decreasing trends, most notable during spring. Major downward trends starting from the last decades of the 19th century are observed during autumn, but only in the Greater Alpine Region, shrinking to a few decades for Germany. During summer, there are major decreasing trends since the mid-20th century for both regions.
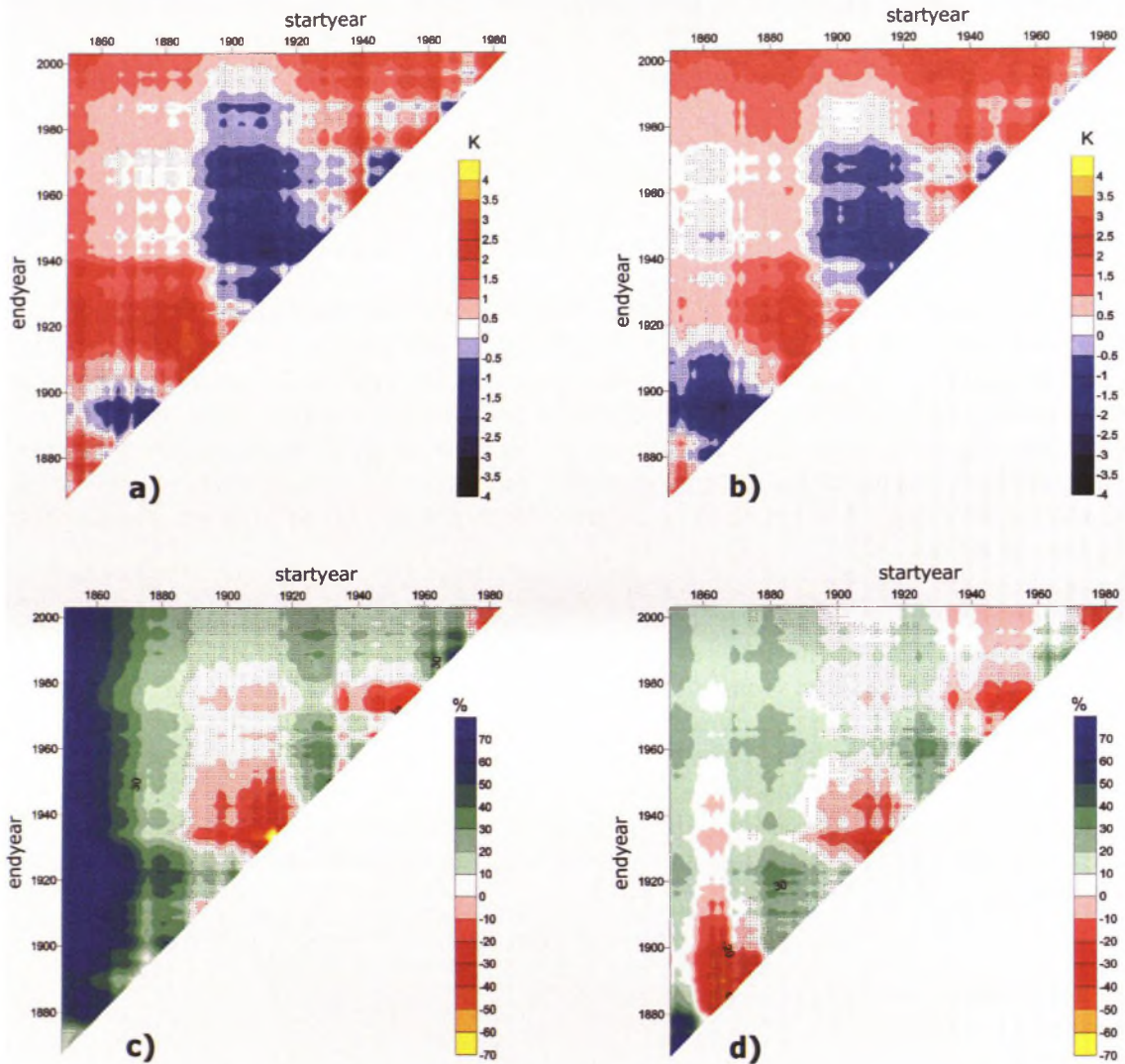
Fig. 5: Winter (DJF) trend matrices for daily mean temperature (a and b) and daily precipitation (c and d, referring to the overall mean of the 1850-2003 period) for the region of Germany (a and c) and the Greater Alpine region (b and d). Statistically insignificant trends (95% level) are indicated by dots.
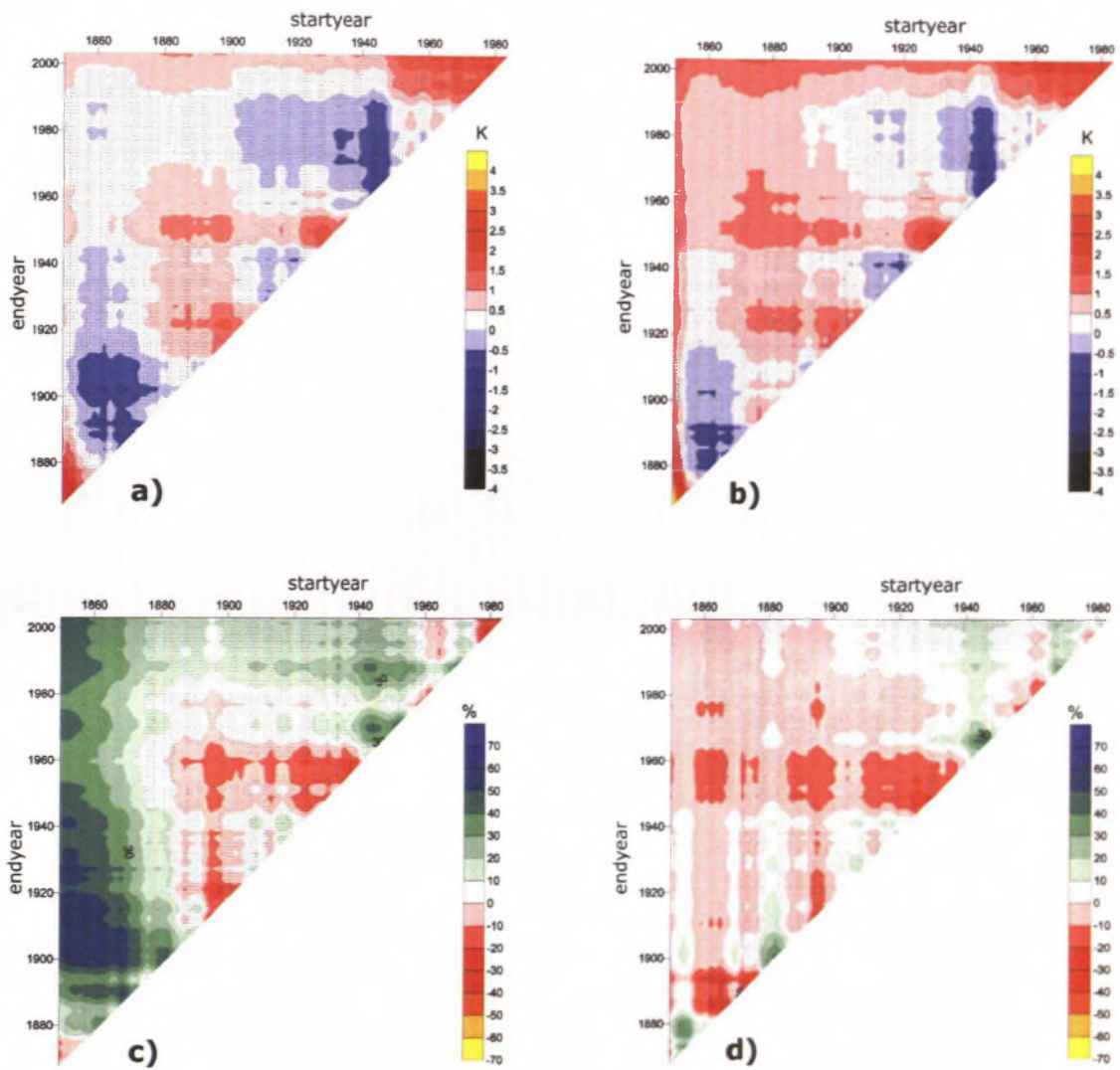
Fig. 6: Spring (MAM) trend matrices for daily mean temperature (a and b) and daily precipitation (c and d, referring to the overall mean of the 1850-2003 period) for the region of Germany (a and c) and the Greater Alpine region (b and d). Statistically insignificant trends (95% level) are indicated by dots.
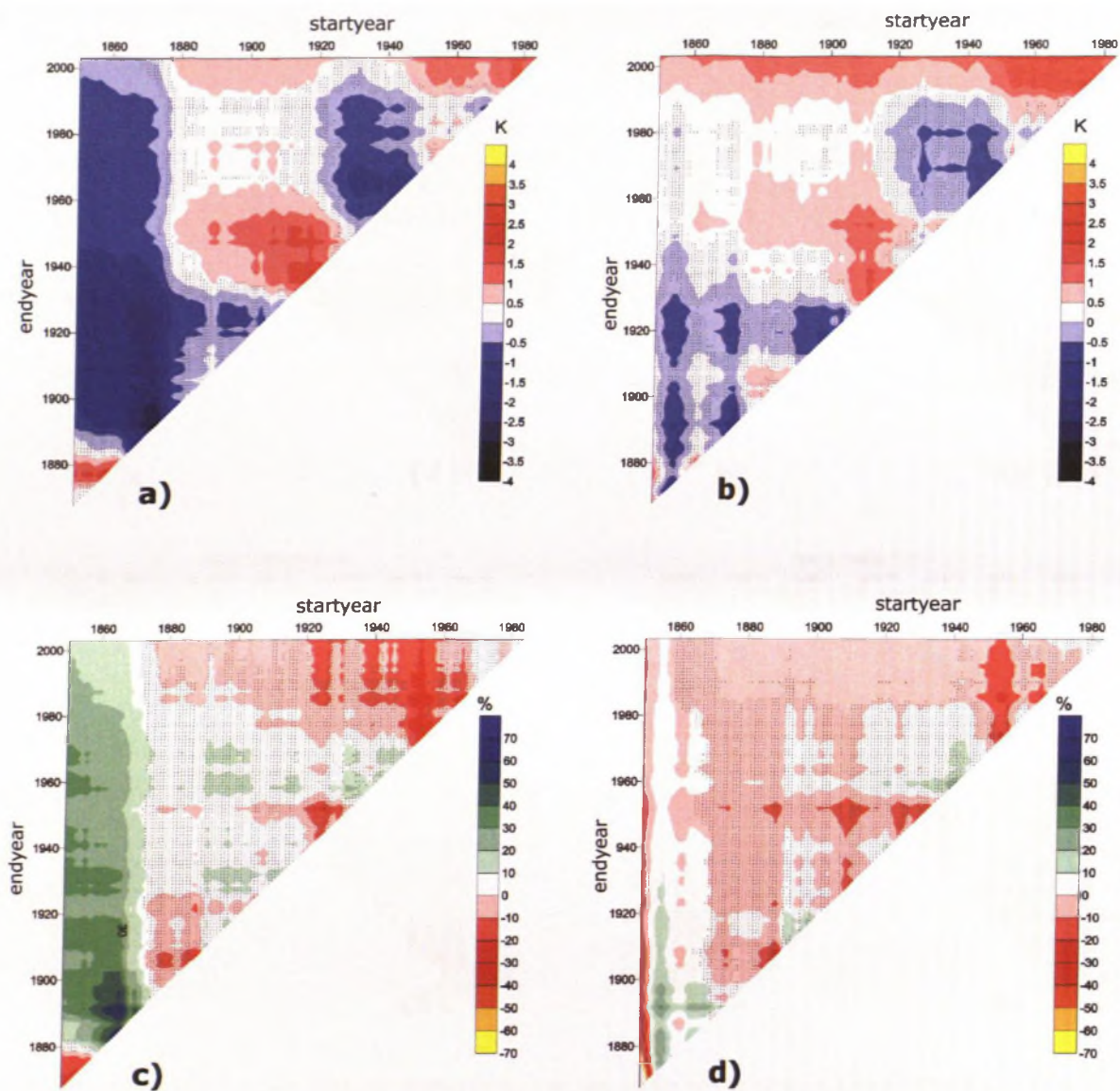
Fig. 7: Summer (JJA) trend matrices for daily mean temperature (a and b) and daily precipitation (c and d, referring to the overall mean of the 1850-2003 period) for the region of Germany (a and c) and the Greater Alpine region (b and d). Statistically insignificant trends (95% level) are indicated by dots.
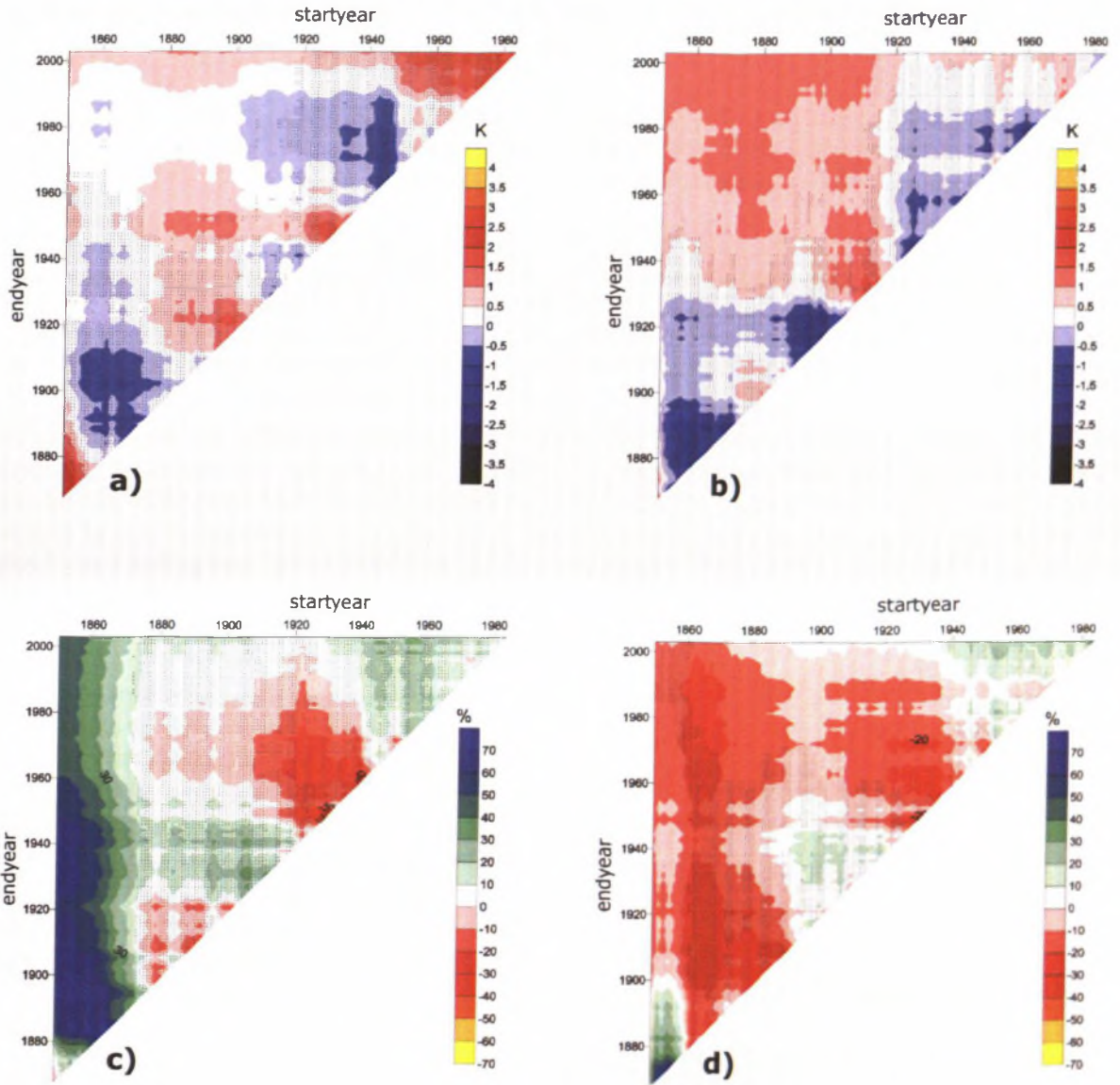
Fig. 8: Autumn (SON) trend matrices for daily mean temperature (a and b) and daily precipitation (c and d, referring to the overall mean of the 1850-2003 period) for the region of Germany (a and c) and the Greater Alpine region (b and d). Statistically insignificant trends (95% level) are indicated by dots.

3.4 Extremes Indices

EMULATE has used 64 different extremes indices. Not all of them are really describing extremes as those reflecting mean conditions (indices 1 – 3 and 56, see Table 1) or individual quantities of any scale (indices 4, 63 and 64). However, they are meaningful as references and therefore included in the set of extremes indices. Some of them are percentiles themselves, whereas other ones are percentile-based. All percentiles have been computed using the following formula:

$$PERC = \frac{(100 - q) * x_k + q * x_{k+1}}{100}; with \ k = \text{int}(\frac{n * q}{100})$$

q is the particular percentile (e.g. the 90th) and n the sample size. x_k and x_{k+1} are two neighbouring positions within the corresponding series sorted in ascending order. This empirical approach is described in more detail for example by Bahrenberg et al. (1990, p. 41).

The extremes indices 5 – 25 (see Table 1) are actual percentiles calculated for a particular season (e.g. for JJA with a sample size of 92 days). The 10th and 90th percentiles do not reflect really extreme conditions, but they are included for the sake of comparisons with more distinct deviations from mean conditions as represented by lower and higher order percentiles, respectively.

For all the remaining percentile-based indices a particular reference percentile has been computed from a pre-defined base-period (1961-1990). By this way 365 reference percentiles (1 per day) using a 5-day window (centred on the particular day of interest) have been computed throughout the whole base-period. Each reference percentile has been calculated from a sample size of 5 days x 30 years = 150 values. All the 29th of February in leap years within the base-period have been included in the reference for the 28th of February. In these cases the sample size increases to 157 (7 leap years in base-period).

An overall missing-value criterion has been applied: up to one missing value per month has been accepted, with a higher rate of missing values the particular index has not been calculated. Indices have been determined for both the four traditional seasons (DJF, MAM, JJA, SON) and the 12 overlapping two-month seasons (JF, FM, MA, AM, MJ, JJ, JA, AS, SO, ON, ND, DJ). A complete list of all 64 extremes indices is described below and shown in Table 1. Indices 63 (FD) and 64 (GSL) have an annual resolution in contrast to the seasonal ones of indices 1 – 62.

Extremes Indices:

1. Mean daily minimum temperature (*MEANTN*)

• $$MEANTN_j = \sum_{i=1}^{N}(TN_{ij}) \Big/ N$$

• Let TN_{ij} be the daily minimum temperature for day i of period j. N is the total number of days during period j.

2. Mean daily maximum temperature (*MEANTX*)

• $$MEANTX_j = \sum_{i=1}^{N}(TX_{ij}) \Big/ N$$

• Let TX_j be the daily maximum temperature for day i of period j. N is the total number of days during period j.

3. Mean daily mean temperature (*MEANTG*)

• $$MEANTG_j = \sum_{i=1}^{N}(TG_{ij}) \Big/ N$$

• Let TG_{ij} be the daily mean temperature for day i of period j. N is the total number of days during period j.

4. Precipitation Total (*PRECTOT*)

- $$PRECTOT_j = \sum_{i=1}^{N}(PREC_{ij})$$

- Let $PREC_{ij}$ be the daily precipitation for day i of period j. N is the total number of days during period j.

5. – 10. Daily minimum temperature percentiles (*TNxP*)
5. 2nd percentile of daily minimum temperatures *(TN2P)*
6. 5th percentile of daily minimum temperatures *(TN5P)*
7. 10th percentile of daily minimum temperatures (TN10P)
8. 90th percentile of daily minimum temperatures *(TN90P)*
9. 95th percentile of daily minimum temperatures *(TN95P)*
10. 98th percentile of daily minimum temperatures *(TN98P)*

11. – 16. Daily maximum temperature percentiles (*TXxP*)
11. 2nd percentile of daily maximum temperatures *(TX2P)*
12. 5th percentile of daily maximum temperatures *(TX5P)*
13. 10th percentile of daily maximum temperatures *(TX10P)*
14. ` 90th percentile of daily maximum temperatures *(TX90P)*
15. 95th percentile of daily maximum temperatures *(TX95P)*
16. 98th percentile of daily maximum temperatures *(TX98P)*

17. – 22. Daily mean temperature percentiles (*TGxP*)
17. 2nd percentile of daily mean temperatures *(TG2P)*
18. 5th percentile of daily mean temperatures *(TG5P)*
19. 10th percentile of daily mean temperatures *(TG10P)*
20. 90th percentile of daily mean temperatures *(TG90P)*
21. 95th percentile of daily mean temperatures *(TG95P)*
22. 98th percentile of daily mean temperatures *(TG98P)*

23. – 25. Precipitation percentiles (*PRECxP*)
23. 90th percentile of daily precipitation amount *(PREC90P)*
24. 95th percentile of daily precipitation amount *(PREC95P)*
25. 98th percentile of daily precipitation amount *(PREC98P)*

26. – 31. Number of events exceeding/falling below
daily minimum temperature (T_{min}) percentiles (*TNxN*)
- using reference percentile from base period (by default: 1961-1990)
26. number of events < 2nd percentile of T_{min} *(TN2N)*
27. number of events < 5th percentile of T_{min} *(TN5N)*
28. number of events < 10th percentile of T_{min} *(TN10N)*
29. number of events > 90th percentile of T_{min} *(TN90N)*
30. number of events > 95th percentile of T_{min} *(TN95N)*
31. number of events > 98th percentile of T_{min} *(TN98N)*

32. – 37. Number of events exceeding/falling below
daily maximum temperature (T_{max}) percentiles (*TXxN*)
- using reference percentile from base period (by default: 1961-1990)
32. number of events < 2nd percentile of T_{max} *(TX2N)*
33. number of events < 5th percentile of T_{max} *(TX5N)*

34.   number of events < 10th percentile of T$_{max}$ (*TX10N*)
35.   number of events > 90th percentile of T$_{max}$ (*TX90N*)
36.   number of events > 95th percentile of T$_{max}$ (*TX95N*)
37.   number of events > 98th percentile of T$_{max}$ (*TX98N*)

38. – 43. Number of events exceeding/falling below daily mean temperature (T$_{mean}$) percentiles (*TGxN*)

- using reference percentile from base period (by default: 1961-1990)

38.   number of events < 2nd percentile of T$_{mean}$ (*TG2N*)
39.   number of events < 5th percentile of T$_{mean}$ (*TG5N*)
40.   number of events < 10th percentile of T$_{mean}$ (*TG10N*)
41.   number of events > 90th percentile of T$_{mean}$ (*TG90N*)
42.   number of events > 95th percentile of T$_{mean}$ (*TG95N*)
43.   number of events > 98th percentile of T$_{mean}$ (*TG98N*)

44. – 52. Particular precipitation extremes indices (*RxN, RxT, RxAM*)

- using reference percentile from base period (by default: 1961-1990)

44.   number of events > 90th percentile of precipitation (*R90N*)
45.   % of total rainfall from events > 90th percentile (*R90T*)
46.   precipitation total from events > 90th percentile (*R90AM*)
47.   number of events > 95th percentile of precipitation (*R95N*)
48.   % of total rainfall from events > 95th percentile (*R95T*)
49.   precipitation total from events > 95th percentile (*R95AM*)
50.   number of events > 98th percentile of precipitation (*R98N*)
51.   % of total rainfall from events > 98th percentile (*R98T*)
52.   precipitation total from events > 98th percentile (*R98AM*)

53. – 55. Mean precipitation from events > x long-term percentile (*SDIIxP*)

- modified Simple Daily Intensity Index (see 56.)

- $$SDIIxP_j = \sum_{i=1}^{E}(PREC_{ij})\bigg/E$$

- Let *PREC$_{ij}$* be the daily precipitation amount on wet days *i* (>= 1mm by default) of period *j* exceeding the long-term xth percentile. *E* is the total number of percentile exceedings during period *j*.
- Long-term percentiles are calculated for a predefined base period (by default: 1961-1990)

53.   mean precipitation amount from events > 90th long-term percentile (*SDII90P*)
54.   mean precipitation amount from events > 95th long-term percentile (*SDII95P*)
55.   mean precipitation amount from events > 98th long-term percentile (*SDII98P*)

56. Simple Daily Intensity Index (*SDII*)

- $$SDII_j = \sum_{i=1}^{N}(PREC_{ij})\bigg/N$$

- Let *PREC$_{ij}$* be the daily precipitation amount on wet days *i* (>= 1mm by default) of period *j*. *N* is the total number of wet days during period *j*.

57. Greatest 5-day total rainfall (*R5d*)

- greatest rainfall amount falling on 5 consecutive days during the period of interest

58. Greatest 1-day total rainfall (*R1d*)

28

- greatest rainfall amount measured on a single day during the period of interest

59. Number of consecutive dry days (*CDD*)
- maximum number of consecutive days with precipitation amount falling below a predefined threshold (by default: < 1mm)

60. Heat Wave Duration Index (*HWDI*)
- total number of at least 6 consecutive days with $Tx_{ij} > Tx_{inorm} + 5\,°C$

- Let Tx_{ij} be the daily maximum temperature at day i of period j. Let Tx_{norm} be the calendar-day mean calculated for a 5 day window centred on each calendar day during a specific base period (by default: 1961-1990).

61. Warm Spell Duration Index (*WSDI90*)
- total number of at least 6 consecutive days with T_{max} exceeding the long-term 90th percentile (long-term: by default 1961-1990)

62. Cold Spell Duration Index (*CSDI10*)
- total number of at least 6 consecutive days with T_{min} below the long-term 10[t] percentile (long-term: by default 1961-1990)

63. Number of frost days during one year (*FD*)
- number of days with $TN < 0\,°C$ during one year

64. Growing season length (*GSL*)
- number of days between the first spell of the year of more than five days with $T_{mean} > threshold$ and the first autumn-winter-spell of the year of more than five days with $T_{mean} < threshold$ (threshold by default: 5°C)

Tab. 1: EMULATE Extremes Indices

No.	Identifier	Parameter	Unit
1	MEANTN	Mean daily minimum temp.	°C
2	MEANTX	Mean daily maximum temp.	°C
3	MEANTG	Mean daily mean temp.	°C
4	PRECTOT	Precipitation total	mm
5	TN2P	Tmin 2nd percentile	°C
6	TN5P	Tmin 5th percentile	°C
7	TN10P	Tmin 10th percentile	°C
8	TN90P	Tmin 90th percentile	°C
9	TN95P	Tmin 95th percentile	°C
10	TN98P	Tmin 98th percentile	°C
11	TX2P	Tmax 2nd percentile	°C
12	TX5P	Tmax 5th percentile	°C
13	TX10P	Tmax 10th percentile	°C
14	TX90P	Tmax 90th percentile	°C
15	TX95P	Tmax 95th percentile	°C
16	TX98P	Tmax 98th percentile	°C
17	TG2P	Tmean 2nd percentile	°C
18	TG5P	Tmean 5th percentile	°C

19	TG10P	Tmean 10th percentile	°C
20	TG90P	Tmean 90th percentile	°C
21	TG95P	Tmean 95th percentile	°C
22	TG98P	Tmean 98th percentile	°C
23	PREC90P	Precipitation 90th percentile	mm
24	PREC95P	Precipitation 95th percentile	mm
25	PREC98P	Precipitation 98th percentile	mm
26	TN2N	no. events < Tmin 2nd percentile	days
27	TN5N	no. events < Tmin 5th percentile	days
28	TN10N	no. events < Tmin 10th percentile	days
29	TN90N	no. events > Tmin 90th percentile	days
30	TN95N	no. events > Tmin 95th percentile	days
31	TN98N	no. events > Tmin 98th percentile	days
32	TX2N	no. events < Tmax 2nd percentile	days
33	TX5N	no. events < Tmax 5th percentile	days
34	TX10N	no. events < Tmax 10th percentile	days
35	TX90N	no. events > Tmax 90th percentile	days
36	TX95N	no. events > Tmax 95th percentile	days
37	TX98N	no. events > Tmax 98th percentile	days
38	TG2N	no. events < Tmean 2nd percentile	days
39	TG5N	no. events < Tmean 5th percentile	days
40	TG10N	no. events < Tmean 10th percentile	days
41	TG90N	no. events > Tmean 90th percentile	days
42	TG95N	no. events > Tmean 95th percentile	days
43	TG98N	no. events > Tmean 98th percentile	days
44	R90N	no. events > Prec. 90th percentile	days
45	R90T	Fraction above Prec. 90th perc.	%
46	R90AM	Prec. total above 90th percentile	mm
47	R95N	No. events > Prec. 95th percentile	days
48	R95T	Fraction above Prec. 95th perc.	%
49	R95AM	Prec. total above 95th perc.	mm
50	R98N	no. events > Prec. percentile	days
51	R98T	Fraction above Prec. 98th perc.	%
52	R98AM	Prec. total above 98th percentile	mm
53	SDII90P	Daily intensity above 90th perc.	mm
54	SDII95P	Daily intensity above 95th perc.	mm
55	SDII98P	Daily intensity above 98th perc.	mm
56	SDII	Simple daily intensity index	mm
57	R5d	Greatest 5-day total rainfall	mm
58	R1d	Greatest 1-day total rainfall	mm
59	CDD	Number of consecutive dry days	days
60	HWDI	Heat wave duration index	days
61	WSDI90	Warm spell duration index	days
62	CSDI10	Cold spell duration index	days
63	FD	Number of frost days	days
64	GSL	Growing season length	days

3.5 Avoiding inhomogeneities at the beginning and at the end of the base-period for reference percentiles

The use of a base-period for computing reference percentiles may cause inhomogeneities in index time-series that count the number of days when a climatic variable exceeds a percentile-based threshold (Zhang et al. 2004). Such threshold-exceedance counts for a particular year in the base-period may be biased if data from the same year is included in the sample from which the percentile is estimated. This may lead to inhomogeneities at the beginning and at the end of the base-period. To minimize this problem, Zhang et al. (2004) developed a special bootstrap technique which has also been used in EMULATE. The whole base-period (1961-1990) is divided into one "out-of-base" year (for which the exceedance will be estimated) and the "almost-complete-base-period" (the remaining 29 years constituting the sample from which the percentiles are estimated). To obtain a complete 30-year base-period, one year of the remaining 29 years will be duplicated. The resulting 30-year-period is then used to estimate percentiles. This procedure is repeated for each of the remaining 29 years – each time leading to a slightly different sample and hence slightly different percentiles. The final reference percentile for the "out-of-base" year is computed by averaging the 29 estimates. This procedure has to be repeated for each single day during the whole base-period. By doing so, one individual reference percentile for each single day during the base-period is obtained. Threshold-exceedance counts for years outside the base-period have been made without this resampling technique. The bootstrap method has been applied to all extremes indices counting exceedances or underruns of reference percentiles computed from the base-period (i.e. indices 26 - 55 and 61 - 62).

3.6 Time series of extremes indices

Time series of 31-year moving frequencies of extreme days, according to the above-mentioned percentile-based indices, have been calculated in order to identify particular periods of increased extreme-day occurrence. The example of Fig. 9, referring to the Central European region of "Germany" (see section 3.3), depicts a strong increase of high-temperature extremes during winter in the recent decades, similar tendencies are observed for precipitation extremes.
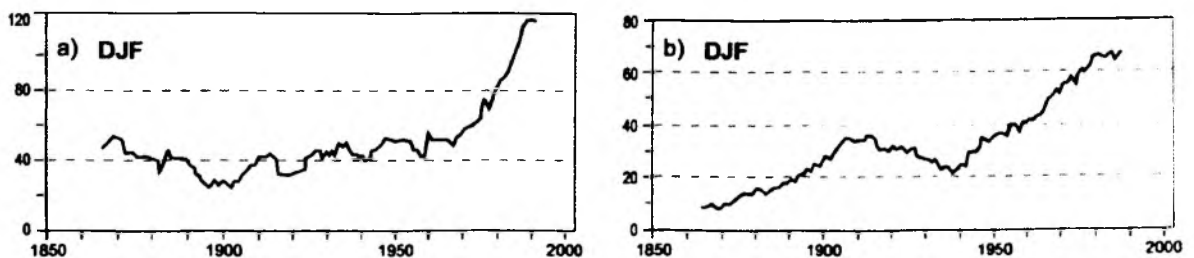
Fig. 9: 31-year moving frequencies of Central European extreme warm days (a) and extreme daily precipitation (b) (beyond the 98th percentile) during winter (DJF) 1850-2003.

Further examples are published by Jacobeit et al. (2009), and a comprehensive documentation of trends in the EMULATE extremes indices has been compiled by Chen et al. (2007). Finally, spatial distributions of index values have been mapped for example by Walther (2004).

4 Summary of the German contribution to Workpackage 2: Derive a set of characteristic atmospheric circulation patterns, and study their variations and trends for each season

4.1 Objectives

The objectives of Workpackage 2 include 4 major issues:

- Define leading atmospheric circulation patterns for two-month and three-month seasons.
- Create a database of quantitative changes in pattern amplitudes since 1850.
- Assessments of trends in pattern amplitudes and in the incidence of their extremes.
- Characterise within-pattern variability.

4.2 Methodology and scientific achievements related to WP2 including contributions from partners

Besides the WP leader from Augsburg (UAUGS), further partners have contributed to WP2, in particular the Hadley Centre (MET OFFICE), the University of Berne (UBERN) and the external expert Ian Jolliffe (Universities of Aberdeen and Reading). This section addresses leading atmospheric circulation patterns (already derived for earlier reports as Deliverable D5), some improvements to the pattern amplitudes (compared to the original version submitted as Deliverable D6), comprehensive trend analyses (satisfying Deliverable D10), studies of within-pattern variability and some further related dynamical aspects.

a) <u>Leading atmospheric circulation patterns</u> have been defined by a novel approach combining simulated annealing clustering with randomizations of the initial partitions in multistart-runs as well as randomizations of the ordering of objects and cluster numbers throughout the iterative reassignments of objects to clusters. These techniques and results concerning long-term variability of corresponding pressure patterns are described in detail in the paper by Philipp et al. (2007) and need not to be repeated in this context. Further results concerning original pattern amplitudes and analyses of overlapping two-month seasons can be obtained from the EMULATE websites.

b) The time coefficients of the mean sea level pressure (MSLP) cluster patterns (the <u>pattern amplitudes</u> according to Deliverable D6) have originally been calculated as correlation coefficients between the cluster centroids and each daily pressure patterns (see the second annual report on the EMULATE website). It turned out that all these coefficients tend to be high obscuring differences between the various cluster patterns (due to correlating raw MSLP patterns with non-orthogonal sets of raw MSLP cluster centroids derived from error- and latitude-weighted pressure fields). Significant improvements have been achieved at UAUGS by calculating Euclidean distances between each daily pressure pattern and the cluster centroids, both being error- and latitude-weighted. These distances in terms of inverted and normalised time series have been submitted as a supplement to D6. Fig. 10 comparing original and novel coefficients for a summer example clearly demonstrates the increased differences between pattern coefficients for the Euclidean-based time series.

c) Major parts of work during the final period of EMULATE were related to Deliverable D10: "<u>Assessments of trends</u> in pattern amplitudes and in the incidence of amplitude extremes". Time coefficients of the cluster patterns based on (non-inverted) Euclidean distances were used as pattern amplitudes (increasing values for growing dissimilarities with the corresponding cluster

centroids), and their extremes were defined in terms of particular percentiles (2nd, 5th, 10th, 90th, 95th, 98th). Trends within the EMULATE period 1850-2003 have been calculated at UAUGS for the 3-month seasons DJF, MAM, JJA, SON and the overlapping 2-month seasons JF, FM, MA, ..., DJ both for pattern amplitudes (based on moving 20-day periods) and for their extreme percentiles (on a seasonal basis). All trends for periods greater or equal than 20 years have been submitted to the non-parametric Mann-Kendall trend test and integrated into triangular trend matrices (with start- and end-year on both axes and the shortest (20-year) periods along the diagonal). Results for all cluster patterns during all 16 seasons and for the 2nd and 98th percentiles have been put on the EMULATE website; some few examples are compiled for the Augsburg website http://geo21/emulate.

Concerning the <u>pattern amplitudes,</u> Fig. 11 shows the trend matrices for two patterns during winter (DJF). Cluster 1 (a NAO-like pattern, see EMULATE webpage or Philipp et al. 2007) has negative distance-trends (i.e. an increase in patterns similar to the centroid) mainly during the last decades; during earlier periods (e.g. ~1910-1970 or from 1860 onwards) less importance is indicated. Cluster 6 (with a strong Russian high and an Atlantic low) has a long-term positive trend in Euclidean coefficients throughout the EMULATE period associated with its negative trend in seasonal cluster frequencies (Philipp et al. 2007) indicating a gradual decline for this Russian high pattern after the end of the Little Ice Age.

During summer (JJA, Fig. 12), different cluster trends can be observed: Clusters 2 and 4 with high pressure ridges from the Azores towards northeastern regions depict long-term increases in importance (declining distances), Clusters 5 and 6 with a more retreated subtropical high rather lost some importance (growing distances) except during most recent Concerning the <u>amplitude extremes</u> only some few significant trends can be observed. The above-mentioned decline in the Russian high pattern during winter (Cluster 6) is also reflected in its percentile trends (Fig. 13): increasing ones for the 2nd percentile around 1860-1960 (indicating less distinct realisations of this pattern) as well as for the 98th percentile around 1860-1910 (indicating further growing distances to this pattern). Similar conditions are also indicated for autumn (Cluster 4, 2nd percentile, not shown).

d) In order to characterize <u>within-pattern variability,</u> several parameters (cp. Jacobeit et al. 2003, Beck et al. 2007) have been calculated on a daily basis: a correlation-based approximation for the relative vorticity within the area 40-60°N, 10°W-30°E; an intensity index measuring the pressure gradients between the corresponding centres of action; a cluster-related temperature index based on 14 Central European stations, and a cluster-related precipitation index based on 25 stations from this area. All these indices have been calculated as normalized 31-year moving averages for all the seasonal cluster patterns (included times in the EMULATE WEBSITE). Fig. 14 shows the seasonal vorticity parameter (independently from actual cluster patterns) indicating a recent accumulation of below-average values during winter, spring and summer after an opposite development especially during winter and summer since the late 19th century.
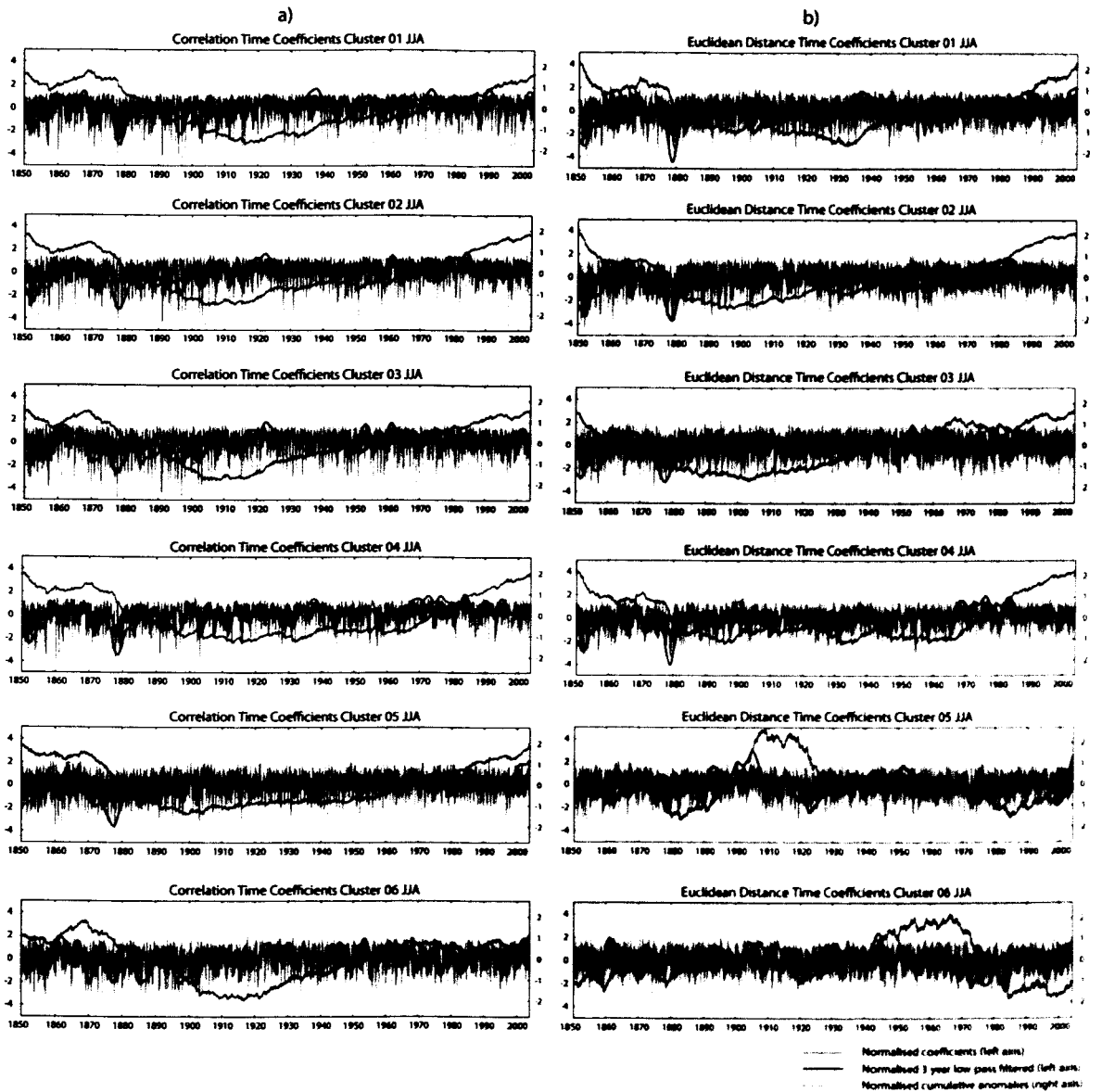
Fig. 10: Different time coefficients for daily mean sea level pressure (MSLP) clusters in summer (JJA) 1850-2003: a) correlation coefficients between each daily pattern and the cluster centroids (grey lines: normalised anomalies, left axis; black solid lines: 3-year low-pass filtered values, left axis; black dashed lines: normalised cumulative anomalies, right axis); b) Euclidean distances (inverted) between each daily pattern and the cluster centroids (grey lines: normalised anomalies, left axis; black solid lines: 3-year low-pass filtered values, left axis; black dashed lines: normalised cumulative anomalies, right axis).

Time coefficients for daily mean sea level pressure (MSLP) clusters in summer (JJA) 1850-2003: a) correlation coefficients between each daily pattern and the cluster centroids (black lines: low-pass filtered, dashed lines: normalised cumulative anomalies); b) Euclidean distances (inverted and normalised) between each daily pattern and the cluster centroids (black lines: low-pass filtered, dashed lines: normalised cumulative anomalies).

35
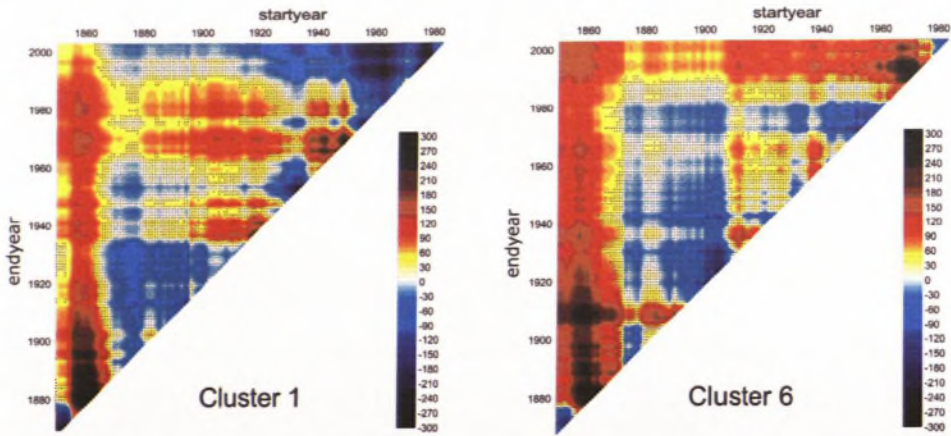
Fig. 11: Winter (DJF) trend matrices for the time coefficients (based on Euclidean distances) of daily MSLP Clusters 1 and 6 (Cluster centroids see Philipp et al. 2007). Statistically insignificant trends (95% level) are indicated by dots.
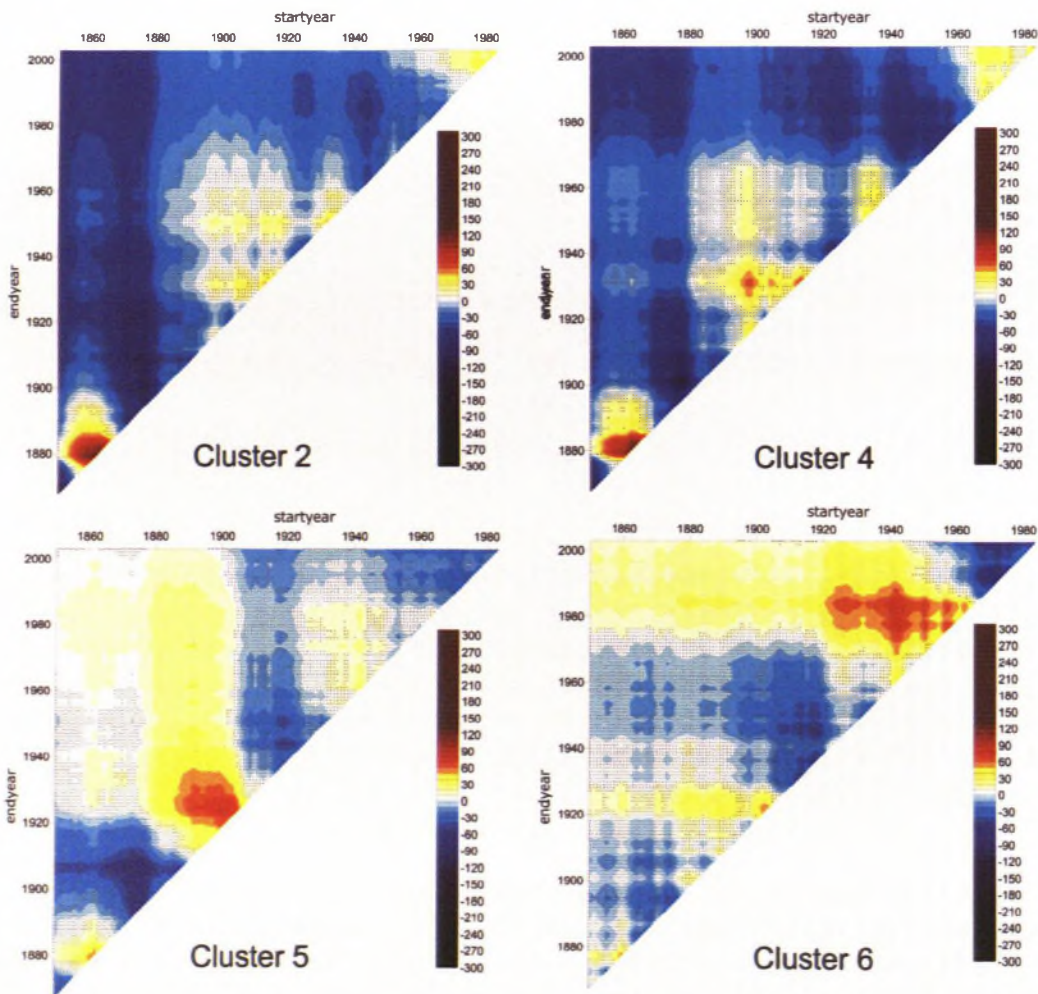
Fig. 12: Summer (JJA) trend matrices for the time coefficients (based on Euclidean distances) of daily MSLP Clusters 2, 4, 5 and 6 (Cluster centroids see Philipp et al. 2007). Statistically insignificant trends (95% level) are indicated by dots.
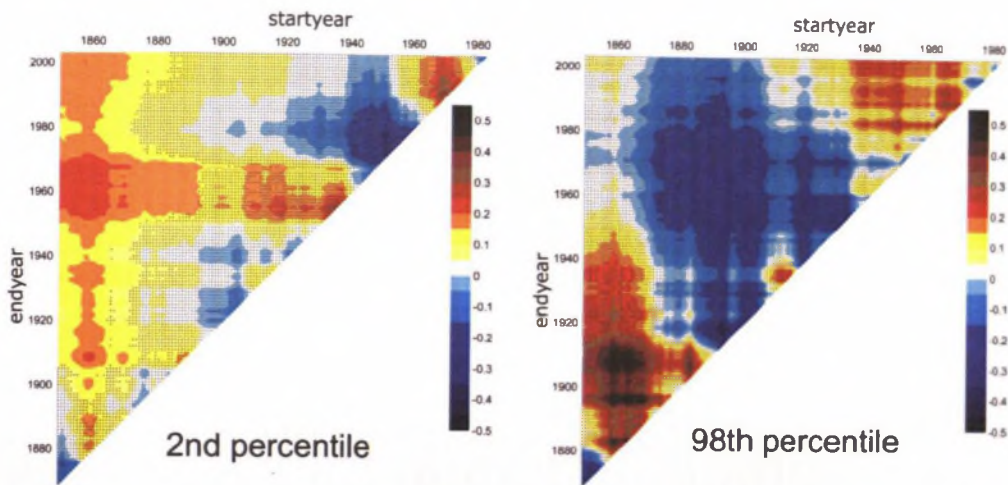
Fig. 13: Winter (DJF) trend matrices of the 2nd and the 98th percentiles of the time coefficients (based on Euclidean distances) of daily MSLP Cluster 6 (Cluster centroid see Philipp et al. 2007). Statistically insignificant trends (95% level) are indicated by dots.
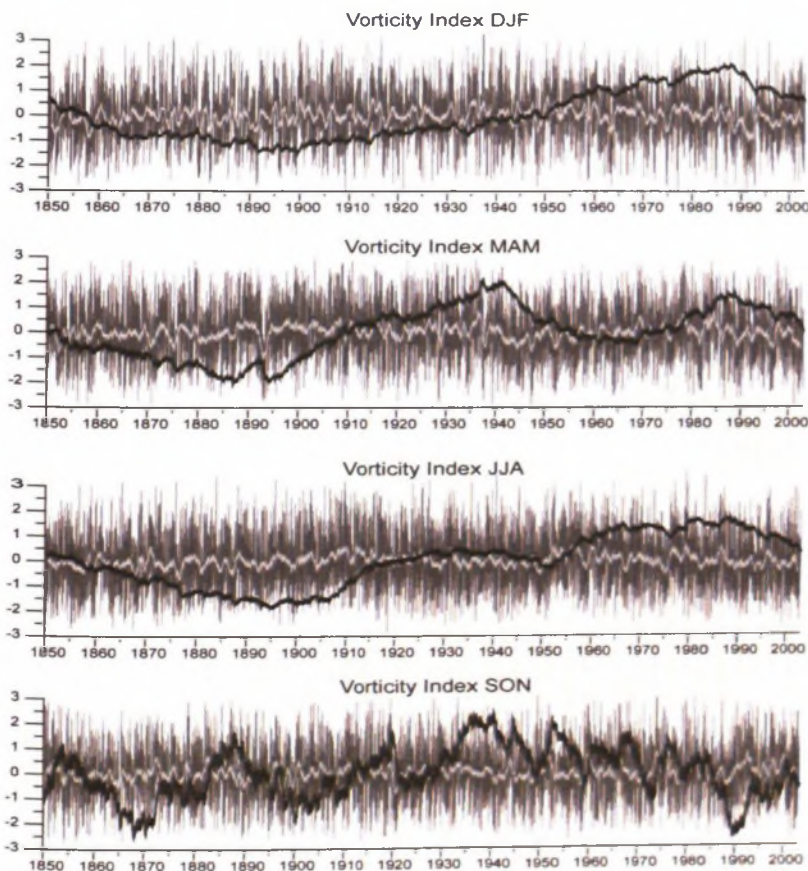
Fig. 14: Normalised Vorticity Index 1850-2003 for the area 40-60°N, 10°W-30°E for winter (DJF), spring (MAM), summer (JJA) and autumn (SON) including 31-year moving averages (white lines) and normalized cumulative anomalies (black lines).
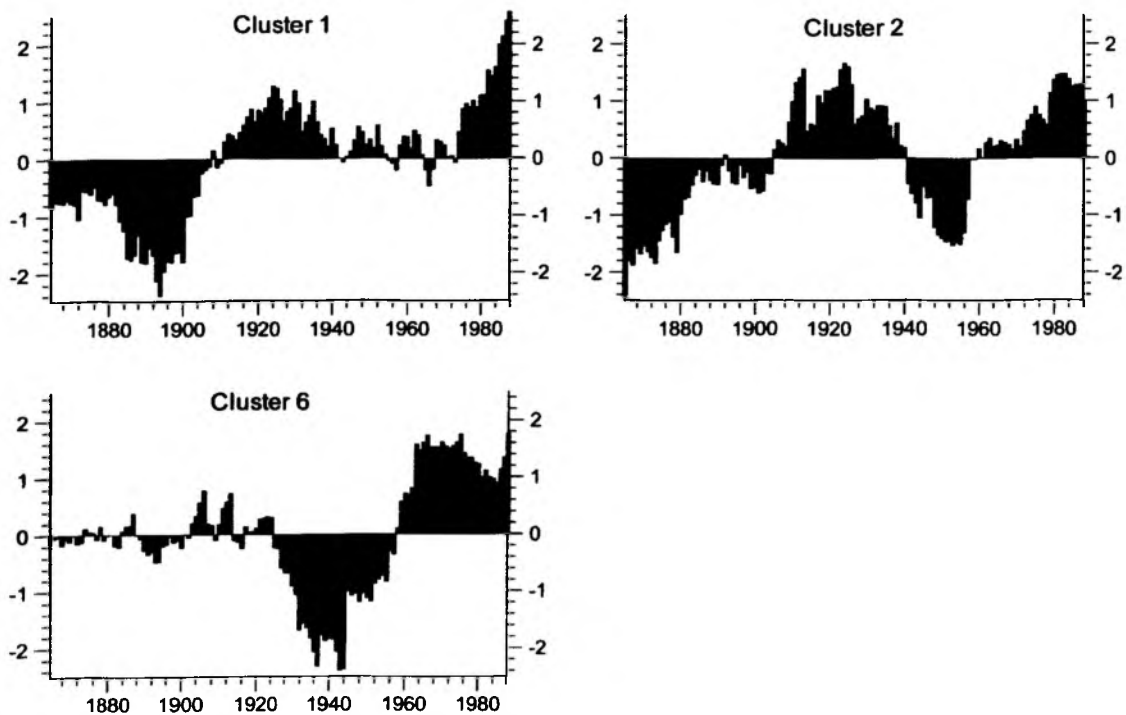
Fig. 15: Normalised 31-year moving averages of within-pattern temperature in Central Europe for daily MSLP Clusters 1, 2 and 6 (Cluster centroids see Philipp et al. 2007) during winter (DJF) 1850-2003.
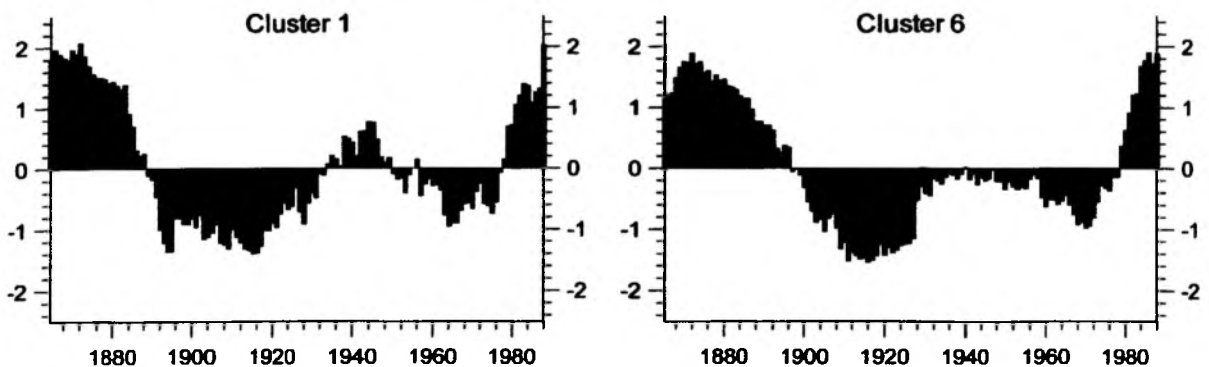
Fig. 16: Normalised 31-year moving averages of within-pattern temperature in Central Europe for daily MSLP Clusters 1 and 6 (Cluster centroids see Philipp et al. 2007) during summer (JJA) 1850-2003.

Concerning within-pattern temperatures, Fig. 15 with 3 cluster examples from winter (DJF) shows a distinct impact of global warming with different degrees of intermediate cooling between ~1930 and 1960: for the NAO-like cluster 1 (see EMULATE website or Philipp et al. 2007) it remains rather moderate, for cluster 2 with a strong Russian high extending up to the British Isles it declines to well below-average values, and for cluster 10 with the Russian high extending only up to Central Europe it develops even stronger before the recent warming which reaches peak values for the west-southwesterly cluster 1.

38

During summer (JJA, Fig. 16), two patterns with low pressure around Iceland (cluster 1) or near Scotland (cluster 6) and only moderate ridging towards Central Europe depict a distinct warm period at the beginning of the EMULATE period turning into a striking cool period during the first decades of the 20th century and starting rather late with 'global warming'. During the transitional seasons, within-pattern temperatures developed quite differently. An example from spring (MAM, Fig. 17) even includes opposite evolutions with a long-term warming throughout the whole period for cluster 2 (low southwest of the British Isles) and a 20th century cooling for cluster 9 (extended high around this region). Detailed studies on regional radiation budgets and boundary conditions would be required to account for such phenomena.
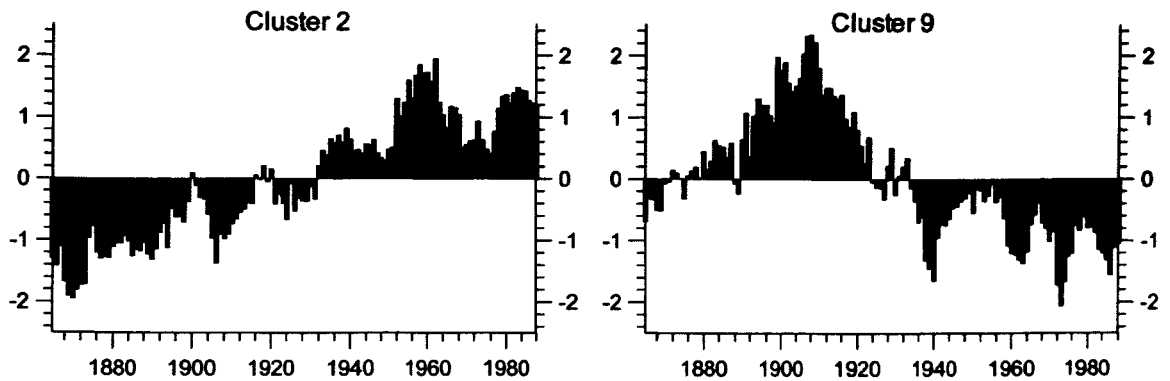
Fig. 17: Normalised 31-year moving averages of within-pattern temperature in Central Europe for daily MSLP Clusters 2 and 9 (Cluster centroids see Philipp et al. 2007) during spring (MAM) 1850-2003.
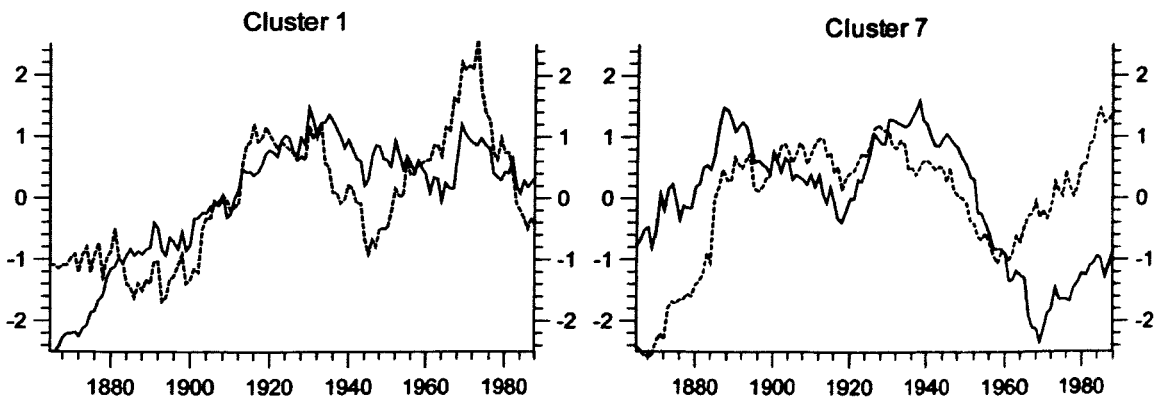
Fig. 18: Normalised 31-year moving averages of within-pattern vorticity for the area 40-60°N/10°W-30°E (gray lines) and within-pattern precipitation in Central Europe (dashed lines) for daily MSLP Clusters 1 and 7 (Cluster centroids see Philipp et al. 2007) during winter (DJF) 1850-2003.

Concerning within-pattern vorticity and precipitation – both indices not always in complete accordance due to different domains, subgrid-scale effects and data restrictions during the earlier periods – the NAO-like cluster 1 for winter shows increases to higher levels since the 1920s with subsequently larger amplitudes for vorticity than for precipitation (Fig. 18). Cluster 7 with a low near Genova has dropped considerably in vorticity since the 1940s, but within-pattern

precipitation turned again already two decades later reaching highest values at the end of the time series (note its calculation as 31-year moving averages). During summer (JJA, Fig. 19) two patterns with marginal high pressure influence in Central Europe (clusters 1 and 5), being rather wet during the 1950s, are drying out since then in connection with increasing anticyclonicity.
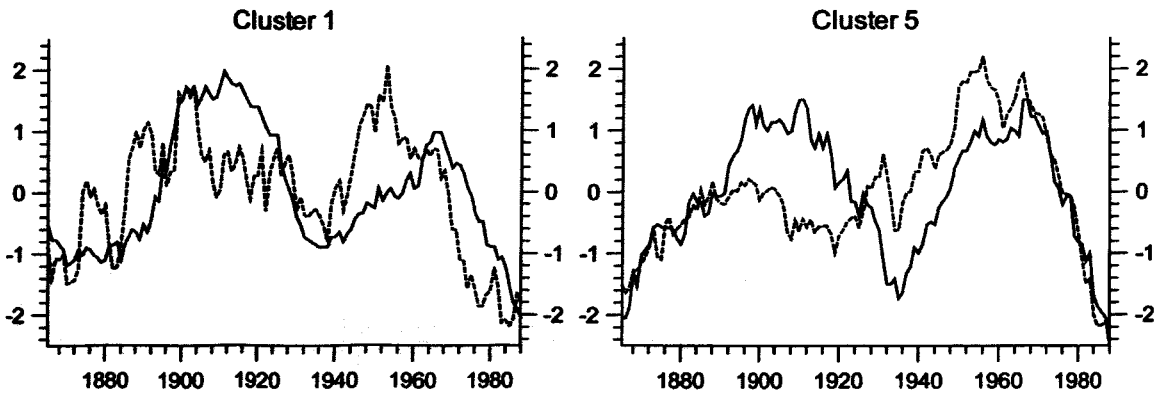
Fig. 19: Normalised 31-year moving averages of within-pattern vorticity for the area 40-60°N/10°W-30°E (gray lines) and within-pattern precipitation in Central Europe (dashed lines) for daily MSLP Clusters 1 and 5 (Cluster centroids see Philipp et al. 2007) during summer (JJA) 1850-2003.

Fig. 20 shows an example of normalised 31-year moving averages of within-pattern temperature and intensity, related to the NAO-like Cluster 1 for winter. Warming of this pattern set in at the end of the 19th century, whereas an increase in within-pattern intensity was not observed before the second half of the 20th century.
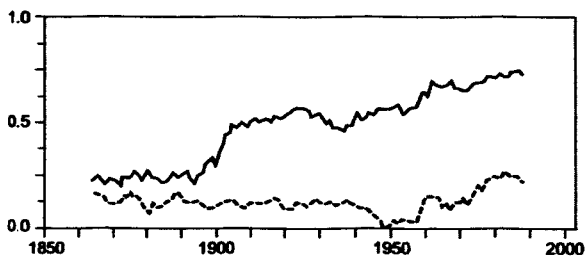
Fig. 20: Normalised 31-year moving averages of within-pattern temperature (black line) and intensity (dashed line) for daily MSLP Cluster 1 (Cluster centroid see Philipp et al. 2007) during winter (DJF) 1850-2003.

e) Finally, additional analyses beyond the scope of defined deliverables were carried out in the context of EMULATE:

In order to derive SLP patterns with particular climatic characteristics (e.g. warm, cold, wet or dry in a selected region), simulated annealing clustering of daily MSLP fields has been performed at UAUGS with temperature or precipitation covariates, respectively. For this purpose station-based indices for Central Europe as already used for within-pattern analyses (section c) have been included, maintaining the (seasonally varying) numbers of clusters from the original MSLP clustering without covariates (see Philipp et al. 2007). Figs. 21 and 22 give two examples for the winter season (DJF) sorting the pressure clusters according to ranked anomalies in climate (note

that this happens intrinsically for precipitation, i.e. clusters with higher (lower) frequencies are always drier (wetter) due to the limited duration of most rainfall events). The thermal MSLP patterns (Fig. 21) with a temperature range of more than 20°C mainly depict a gradual sequence with a retreating Russian high and an increasing NAO. The precipitation-related patterns (Fig. 22) only include three anticyclonic ones with less precipitation (originating from Russian or Azores high pressure influence), the other ones with increasing precipitation are marked by gradually southward penetrating and intensifying cyclonic waves.
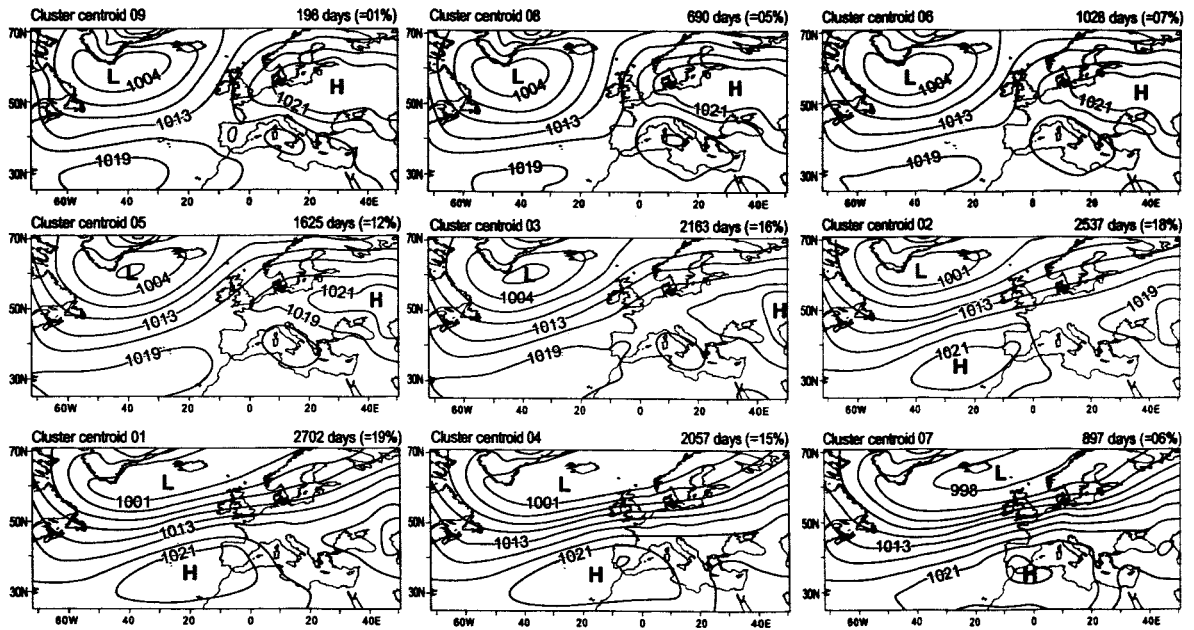
Fig. 21: Centroid patterns of winter (DJF) daily MSLP clusters using Central European temperature as covariate. Clusters are sorted from left to right and from top to bottom according to increasing mean temperatures of the clusters (see Table 1).

Tab. 2: Mean and standard deviation of cluster-related Central European temperature anomalies as well as frequency for the winter (DJF) daily MSLP clusters from Fig. 21.

cluster number	mean temperature anomaly (°C)	standard deviation	frequency in days
09	-13.3	2.155	198
08	-8.6	1.104	690
06	-5.3	0.785	1028
05	-2.9	0.660	1625
03	-0.8	0.588	2163
02	1.2	0.552	2537
01	3.1	0.577	2702
04	5.2	0.687	2057
07	8.0	1.110	897
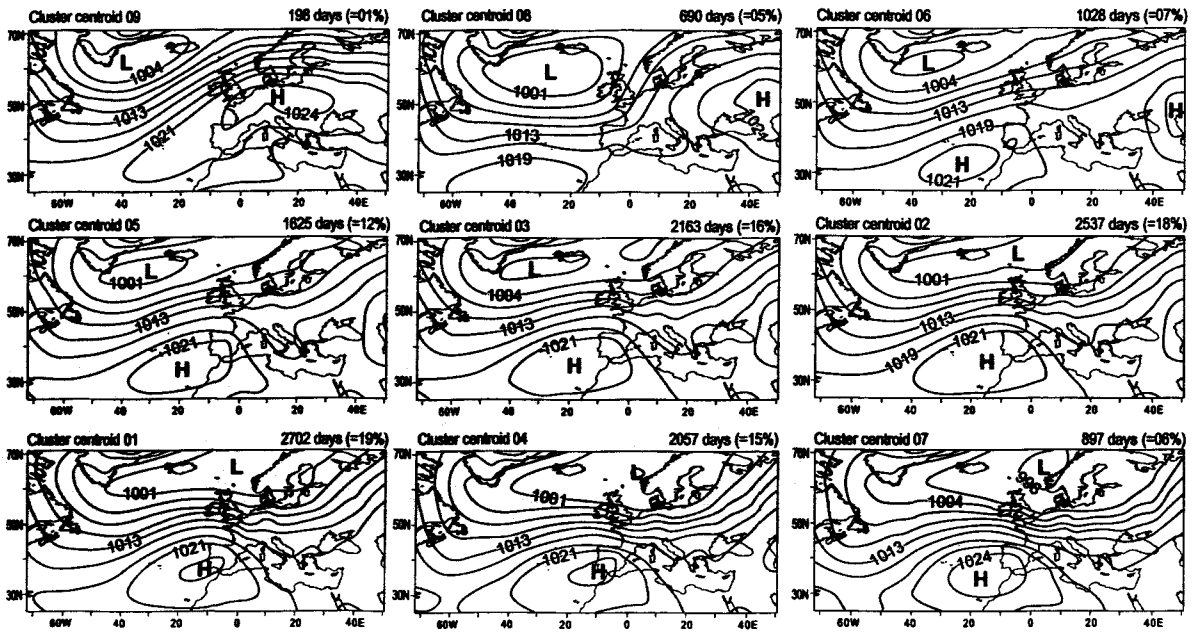
Fig. 22: Centroid patterns of winter (DJF) daily MSLP clusters using Central European precipitation as covariate. Clusters are sorted from left to right and from top to bottom according to increasing mean precipitation of the clusters (see Table 2).

Tab. 3: Mean and standard deviation of cluster-related Central European precipitation anomalies as well as frequency for the winter (DJF) daily MSLP clusters from Fig. 22.

Cluster number	mean precipitation anomaly (mm)	standard deviation	Frequency in days
01	-0.64	0.074	2943
02	-0.63	0.085	2113
03	-0.25	0.120	1725
04	0.20	0.141	1121
05	0.74	0.171	787
06	1.39	0.213	486
07	2.28	0.284	253
08	3.40	0.431	101
09	5.69	0.966	19

In order to present a more comprehensive overview of MSLP patterns included in each cluster, UAUGS followed an idea by Ian Jolliffe (Universities of Aberdeen and Reading) to select – besides the nearest pattern to the centroid – additional patterns being distinctly different from it (in terms of Euclidean distances). This may be achieved by iteratively selecting that pattern whose minimum distance to either the centroid or the earlier selected patterns is the highest one of all remaining patterns. This growing set of 'fringe patterns' is defined to be complete if the distance to any of the predecessors is lower than the half of the maximum diameter of the corresponding cluster. Fig. 23 presents these fringe patterns for the first 3 MSLP clusters during winter (DJF)

42

1850-2003 clearly pointing to significant differences between patterns within the same cluster. For example, the second pattern within cluster 1 does not reproduce a positive mode of the NAO which constitutes the centroid pattern. Thus, considerable within-cluster variability has to be taken into account during each kind of dynamical analysis.
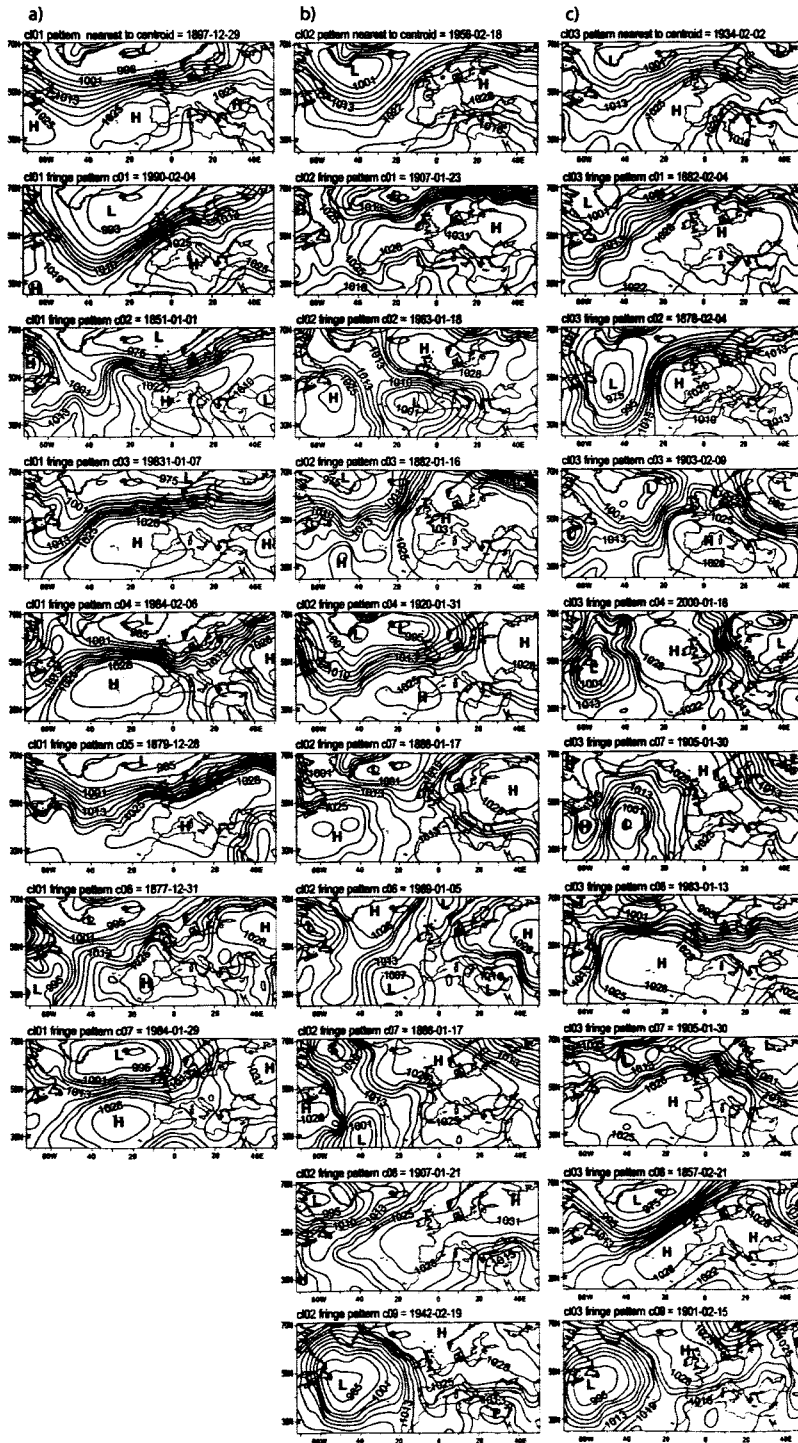
Fig. 23: Daily MSLP patterns representing the range of patterns included within the same cluster for winter (DJF) 1850-2003: a) cluster 1, b) cluster 2, c) cluster 3. The first pattern in each case is the nearest one to the corresponding centroid (see Philipp et al. 2007), the following patterns represent "fringe patterns" being the most different ones to those selected before.

The time constrained clustering developed at UWUERZ/UAUGS according to suggestions of Ian Jolliffe (Universities of Aberdeen and Reading) aiming at an increased persistence in cluster sequences, was further investigated with respect to appropriate rules for adjusting the degree of constraining, but no definite rules could yet be determined. Instead another extended approach in clustering techniques called COSA (clustering objects on subsets of attributes) has been elaborated at UAUGS according to suggestions of Ian Jolliffe. First attempts (not shown) have been made with regional subsets (Central Europe and the Mediterranean area), but no straightforward interpretation of results could be realized until now.

UBERN investigated North Atlantic and European winter cyclone changes for the 1881-2003 period by applying a Lagrangian cyclone tracking algorithm (Murray and Simmonds 1991) on the MSLP dataset (referring to large-scale systems according to the gridded data resolution). Cyclone system density (Fig. 24) has also been computed at grid points north and south of the line connecting 45°N, 60°W with 55°N, 30°W (Bhend 2005) providing a North-Atlantic storm track index (see Fig. 25 with positive values for a northern position). There has been a significant decrease in the number of cyclones in the central North Atlantic and the Mediterranean region from 1881 to 2003 linked with a northward shift of the North Atlantic storm track. However, there are considerable uncertainties remaining in the dataset (increasing number of observations!) especially for the Atlantic region (high RSOI errors!).

Trend of SYSTEM-DENSITY of low in DJF EMSLP including 1881 to 2003
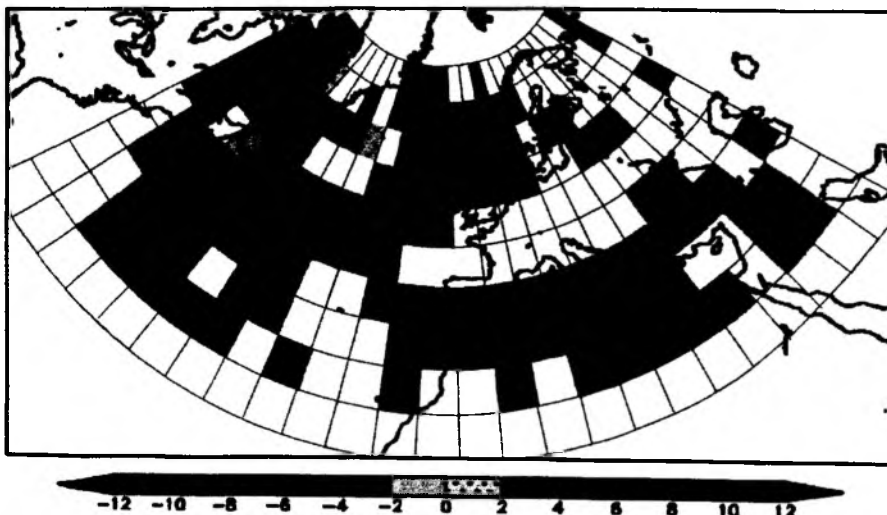
Fig. 24: Linear trends in winter (DJF) cyclone system density for the 1881-2003 period (calculations by Paul Della-Marta).
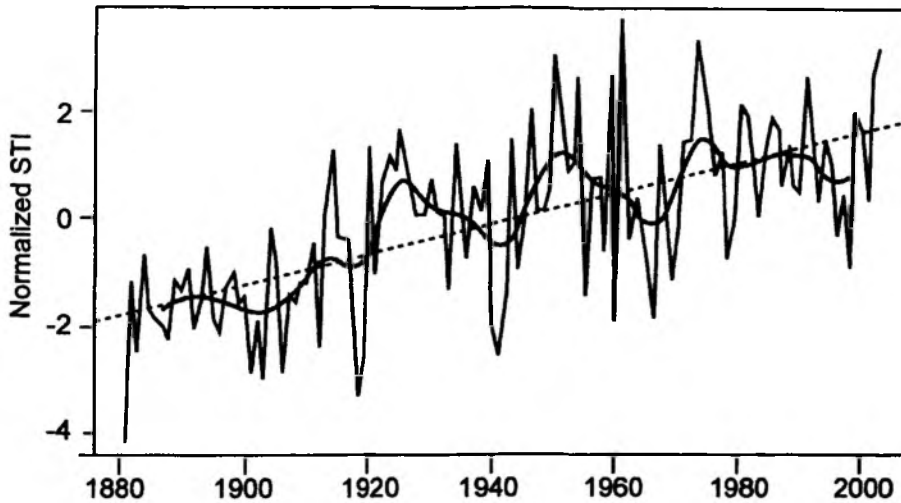
Fig. 25: The winter (DJF) North Atlantic storm track index (STI) for the 1881-2003 period (positive values indicate a northern position), including low-pass filtered time series (gray line) and linear trend line (dashed line) (calculations by Paul Della-Marta).

In order to achieve a closer correspondence of circulation patterns to regional extremes in temperature and precipitation, an objective classification into Central European Grosswettertypes (GWT) that has been derived on a monthly scale (Beck et al. 2007) has been adopted to the daily scale within EMULATE. This classification (Fig. 26) includes ten major types according to the main flow directions (W, SW, ...) and to regional pressure centres (HC: High above Central Europe; LC: Low above Central Europe). It was applied to some of the WP4 analyses (see section 6).
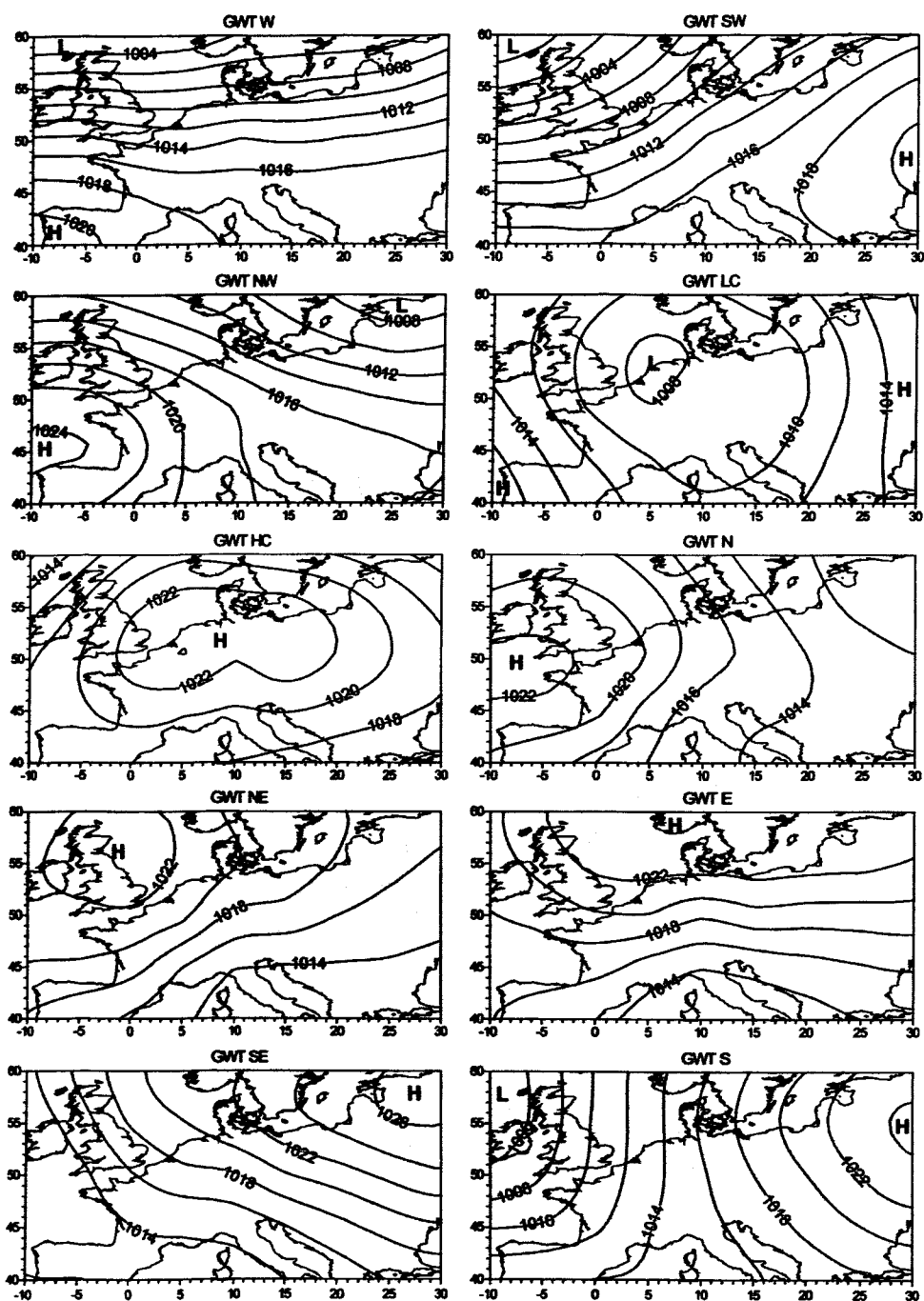
Fig. 26: Daily MSLP composites 1850-2003 for the 10 Central European Großwettertyps (GWT) defined by main flow directions (W, SW, ...) and regional pressure centres (HC: High above Central Europe; LC: Low above Central Europe).

4.3   Socio-economic relevance and policy implications

The classification of daily SLP fields into atmospheric circulation types has been used for studying circulation dynamics of climatic extreme events (link to Workpackage 4), and this will be of major importance for society including risk assessments, adaptation and mitigation strategies.

46

5 Summary of the German contribution to Workpackage 3: Relate variations and trends in atmospheric circulation and associated surface climate variability over Europe to sea surface temperature patterns, particularly from the North Atlantic

Studies on relationships with SSTs have been performed by the Hadley Centre (see EMULATE website), but in context of Deliverable D11 (Assessment of the time-varying influence of SST and atmospheric circulation on European surface temperature and precipitation patterns) further contributions of the German working group on circulation dynamics have been included within Workpackage 3. Thus, this section consists of two different parts: the first one deals with a comparison of daily MSLP clustering between the whole EMULATE period (1850-2003) and three sub-periods (SP1: 1850-1900, SP2: 1901-1951, SP3: 1952-2003), the second one provides temperature and precipitation patterns for the daily MSLP clusters (based on daily station time series from section 3) again including patterns for the whole EMULATE period and for the different sub-periods mentioned above. Some indications are expected about the degree of non-stationarity of climate and MSLP clusters within the EMULATE period. All figures mentioned in section 5 are available from the following Website: http://geo21/emulate/wp3

5.1 Daily MSLP clustering for sub-periods

The same simulated annealing clustering technique used to define leading atmospheric circulation patterns for the whole period 1850-2003 (D5 as part of WP2) was applied to the daily MSLP fields of the sub-periods SP1 to SP3. Results for the 3-month seasons are given at the above-mentioned Website including the principal solutions for the whole 1850-2003 period (Website Figs. 1-4). A high degree of stationarity is indicated if all principal patterns of a particular season can be identified in all sub-periods with only minor variations in frequency or in shape of the centroid patterns. Substantial non-stationarity would be indicated if merging or splitting of particular patterns could be observed for some of the sub-periods.

a)   Winter (DJF) – Fig. 1 at http://geo21/emulate/wp3

All principal patterns are clearly identified during all sub-periods, but there are some remarkable changes in ranking, especially between SP1 and SP2, whereas only minor changes occur during the 20th century. This might indicate some circulation changes from the 19th to the 20th century, but might also reflect different data quality and reconstruction skill.

The first principal pattern resembling the positive mode of the NAO has intermediately dropped down during the first half of the 20th century (only rank 3 in SP2), in accordance with its long-term changes in seasonal cluster frequency (SCF, shown at the Website for the 1850-2003 period within Fig. 5). The pattern itself experiences a strengthening and a north-eastward shift of the Azores High whereas no major change is indicated for the Icelandic Low.

The second principal pattern showing no long-term trend in SCF, occurs as sixth cluster in SP1 and as first cluster afterwards. This change is linked with a distinct shift of the anticyclonic centre from Russia (19th century) to the Baltic area (20th century). At the same time a similar pattern concerning the eastern high pressure influence (number 6 in the 1850-2003 period) decreases from rank 3 (SP1) to rank 8 (SP2 and SP3).

Principal pattern 7 includes a western Mediterranean cut-off cyclone ("Genova low") which is obviously weakened throughout the sub-periods. On the other hand, principal pattern 8

47

proceeding from the last rank (SP1) to the 7th rank (SP2) and to the 5th rank (SP3), represents a deepening of the Genova low, however in conjunction with another dynamical mode characterized by a central North Atlantic low pressure system.

b)   Spring (MAM) – Fig. 2 at http://geo21/emulate/wp3

The degree of stationarity is distinctly lower during this season with only some few cluster patterns being recognised during all sub-periods. This may partly be due to the higher number of clusters implying a higher probability for changes between different sub-periods, but also reflects the larger variability during this transitional season. Furthermore, 5 of the 11 principal patterns of the 1850-2003 period have significant trends in their seasonal cluster frequencies (see Website Fig. 6).

Pattern 1 (blocking high near the British Isles) not only increases in frequency (from 10% in cluster 5 of SP1 to 12% in cluster 3 of SP2 to 16% in cluster 1 of SP3), but also shows a stronger low in the western Atlantic during the 19th century (SP1) than afterwards.

Pattern 2 (low southwest of the British Isles, first cluster in SP1 and SP2, second one in SP3) is deepening in the last sub-period, somewhat similar to Cluster 11 (remaining at the same position).

The fact that Clusters 10 and 11 keep their relative position in contrast to the more frequent ones may confirm that the reorganisation of major clusters during spring is not an artificial one but in fact reflects the enhanced dynamics during this transitional season.

c)   Summer (JJA) – Fig. 3 at http://geo21/emulate/wp3

All principal patterns from the whole period 1850-2003 can clearly be identified during all sub-periods with only minor changes in frequency. Pattern 2 (changing to cluster 1 in SP1) includes a northeastward extension of the Azores High throughout the sub-periods, Pattern 5 (changing to cluster 3 in SP2 and SP3) indicates an intensification of a western Atlantic low.

d)   Autumn (SON) – Fig. 4 at http://geo21/emulate/wp3

Complete correspondence for all patterns is only achieved within the 20th century (i.e. between SP2 and SP3), among the principal patterns from the 1850-2003 period less than one half (numbers 6 to 8) persist throughout all sub-periods (with some changes in ranking). The first 5 clusters, however, are reorganised (merging or splitting) in SP1 and SP2 indicating substantial non-stationarity between the 19th and the 20th centuries.

Altogether there are distinct seasonal differences in the degree of non-stationarity with maxima during the transitional seasons and low levels for summer and winter.

5.2   Temperature and precipitation patterns for the daily MSLP clusters

These patterns are based on daily station time series and calculated for the whole EMULATE period 1850-2003 (departures from the seasonal whole-period mean for each station) as well as for the three sub-periods (departures from the whole-period value for each station). 326 precipitation and 242 temperature records of different lengths are available from Workpackage 4, however only 57 for precipitation and 63 for temperature are indicated as reliable, due to supposed inhomo-geneities according to Della-Marta & Wanner (2006). Nevertheless, all stations were used to

achieve meaningful patterns for the whole period, since the separation into particular anomalies for each pressure pattern seems to be stronger than any artificial bias in the dataset. In addition, temperature patterns based on NCEP/NCAR reanalysis data for the 1948-2003 period are included at the above-mentioned Website (Figs. 5-8). For rainfall, however, results based on NCEP/NCAR daily precipitation rates remained noisy and will not be discussed. Generally, there is a large degree of correspondence between the temperature/rainfall deviations (Website Figs. 9-16) and conditions that are expected from the pressure distributions of the cluster centroids. Thus, only particular phenomena will be addressed in the following.

e)   Winter (DJF) – Figs. 5, 9, 10 at http://geo21/emulate/wp3

The temperature composites for all pressure clusters correspond exactly to those derived from reanalysis data. Some details for the SLP clusters considering the sequence of sub-periods may be specified:

-        Cluster 1 (resembling the positive mode of the NAO) becomes much warmer throughout the sub-periods, SP1 was slightly drier for a majority of stations, SP3 distinctly wetter for most stations.

-        Cluster 2 (High over the Baltic region) has become slightly drier during the last 50 years for most of the Central European stations, the opposite is true for Spain.

-        Cluster 3 has moderately warmed, SP2 was slightly wetter (drier) in Central Europe (Iberia).

-        Clusters 4 and 5 being the wettest ones for Central Europe became mostly wetter and moderately warmer throughout the sub-periods. Great Britain is affected in a different way (positive rainfall anomalies for Cluster 4, negative ones for Cluster 5).
-        Cluster 6 has warmed especially from SP2 to SP3, no distinct changes are indicated for precipitation.
-        Clusters 7 and 8 are mostly dry or normal over Europe except of the Central Mediterranean (Genova Low in Cluster 7) and Spain (negative pressure departures in Cluster 8). Southern Europe was slightly drier with Cluster 8 in SP2.
-        Cluster 9 was unusually cold in the 19. century (SP1), continuously warming on the Iberian peninsula, but already warmest in Central and NE-Europe during SP2. In this period Alpine stations were remarkably wetter.

f)   Spring (MAM) – Figs. 6, 11, 12 at http://geo21/emulate/wp3

During this season some differences appear between temperature patterns based on NCEP/NCAR reanalysis and those based on station data. A prominent one is linked with Cluster 1 showing below-average temperatures in Central Europe for reanalysis data and slightly positive departures for station data (but remaining smaller than in other regions). This should primarily be due to the different mean values used as reference (1948-2003 against 1850-2003). Details for particular pressure patterns may be summarized as follows:

-        Cluster 1 has become wetter in the Alpine region during the last 50 years (SP3).
-        Clusters 2 and 3 showed a distinct warming throughout the whole period.
-        Cluster 4, the wettest in spring, continues to become still wetter.
-        Cluster 6 was unusually warm in the first half of the 20. century (SP2).
-        Clusters 7 and 8 depict a continuous warming.
-        Cluster 11 has become much wetter.

g)   Summer (JJA) – Figs. 7, 13, 14 at http://geo21/emulate/wp3

Temperature composites for the pressure clusters have a very high degree of correspondence between NCEP/NCAR reanalysis and EMULATE station data. Some details for particular pressure patterns may be specified:

-    Clusters 1 and 2 are continuously warming.
-    Cluster 3 was warmest during the first half of the 20· century (SP2).
-    Cluster 4 resembling the positive mode of the summer NAO (according to the NOAA-CPC pattern), has the driest conditions and a long-term positive trend in seasonal cluster frequencies (SCF, Fig. 7).

Summer reveals only minor changes of rainfall departures for the pressure patterns, but a widespread warming tendency.

h)   Autumn (SON) – Figs. 8, 15, 16 at http://geo21/emulate/wp3

There are only minor differences between the temperature composites (reanalysis and station data) for the pressure patterns. Particular details may be summarized as follows:

-    Clusters 1, 2 and 4 depict some warming from SP1 to SP2, Clusters 2 and 4 a subsequent cooling from SP2 to SP3.
-    Cluster 5 has no clear tendency in temperature, but becomes wetter.
-    Cluster 6, the wettest in autumn, continues to become still wetter. Additionally it reveals a strong warming from SP2 to SP3.
-    A similar warming is indicated for Clusters 7 and 8, the former also becoming much drier in Central Europe.

Altogether, there are considerable changes in the temperature and rainfall departures with notable differences between particular pressure patterns. These changes are an important component of climate change (beyond the various changes in frequency of principal pressure patterns), known as within-type changes (see for example Beck et al. 2007).

6 Summary of the German contribution to Workpackage 4: Relate variations and trends in atmospheric circulation patterns to prominent extremes in temperature and precipitation

This section is in context of Deliverable D15 focussing on some aspects of relationships between the atmospheric circulation and the incidence of temperature and precipitation extremes in the Central European region of Germany. One part (sub-section 6.1) is dealing with the different importance for such extremes of circulation patterns derived from daily MSLP classifications, another part (sub-section 6.2) is specifying major circulation patterns linked to such extremes by means of various principal component analyses (for a general discussion of these different tools for studying circulation-climate relationships see for example Jacobeit 2009).

6.1 Daily MSLP classifications in relation to temperature and precipitation extremes

These analyses are based on the above-mentioned daily temperature and precipitation time series for the region of Germany defining extremes by the 2nd, 5th, 10th, 90th, 95th and 98th percentiles for temperature and by the 90th, 95th and 98th percentiles for precipitation. All calculations have been made for 3-month and 2-month seasons, including the three sub-periods (1850-1900, 1901-1951, 1952-2003) in order to record temporal variabilities within the EMULATE period 1850-2003. The large-scale atmospheric circulation will be represented by two different classifications: on the one hand cluster patterns will be used that have been derived from the reconstructed daily MSLP fields (WP1) by simulated annealing techniques developed in WP2 (Philipp et al. 2007). These patterns are also available from the EMULATE website and will only be cited in terms of their seasonal numbers. On the other hand the objective classification into Central European Grosswettertypes (GWT) described in section 4.2 (part e) has been used (see Fig. 26 and Beck et al. 2007). This classification focussing on Central Europe may have a closer correspondence to regional extremes in temperature and precipitation than large-scale patterns which have been derived with respect to the whole North-Atlantic-European region.

For each season and for each of the extreme types defined above, the frequency distributions of days with and without a particular extreme in dependence of the circulation types (cluster patterns as well as GWTs) have been calculated for the 1850-2003 period and the three ~50-year sub-periods. All these 720 diagrams are available from the EMULATE website, this final report includes only some few selected examples (further results being discussed in Jacobeit et al. 2009).

Fig. 27 shows that during the main winter (January/February) season more than 50% of the heavy precipitation events (beyond the 95th percentile) occurred during GWT West. The sub-periods indicate additionally that this dominance has further increased with time (from below 45% during the second half of the 19th century to roughly 57% during the last 50 years). This percentage increase is also stronger than the increase in non-extreme days with GWT West. The second important type for such extremes, GWT Northwest, had its highest fraction during the first half of the 20th century, declining afterwards but still keeping larger percentages for extreme days than for non-extreme days. Generally similar distributions are shown for extremely warm winter days (Fig. 28), but the second most important GWT is now Southwest with increasing percentages of extreme days in the course of the 20th century.

Referring to the cluster classification of circulation patterns (see EMULATE website), there is - beyond a NAO-like pattern - another westerly one with an eastward shifted low pressure centre in higher latitudes (Cluster 6 for the Jan./Feb. season). According to Fig. 29, this pattern has also been important for distinctly positive temperature anomalies (except the last 50 years when the

NAO-like Cluster 1 further increases in predominance). Fig. 30 presents SLP composites for Cluster 6 for two sub-samples: for all extreme days (based on the 1901-1951 period) linked with the occurrence of Cluster 6 members on the one hand and for a random sample with the same size of non-extreme Cluster 6 members on the other hand. Obviously the extreme sample is characterized by an eastward extension of the Azores high pressure and by an westward extension of the North European low pressure, leading to a more zonal configuration than during normal conditions and in particular to enhanced pressure gradients above Central Europe. Similar composites for heavy precipitation events (Fig. 31) do not indicate such a zonalisation, but rather a strengthening of the two pressure centres with a southward extension of the cyclonic wave, leading to decreased pressure by more than 3 hPa above northern Central Europe in comparison to the composite for normal conditions. Fig. 32 confirms that Cluster 6 is most important for strong precipitation during this season, including the most recent sub-period. Thus, in contrast to positive temperature extremes during winter being linked preferably to zonal patterns within the positive mode of the NAO, heavy winter precipitation in Central Europe is distinctly associated with less zonal patterns like in the Cluster-6 extreme-composite (Fig. 31).

Looking at the summer season (JJA), Fig. 33 points to the primary importance for Central European hot days of Cluster 1 patterns (high pressure ridge from the Azores to Scandinavia, see EMULATE website). A second pattern with higher percentages of extreme days than of normal days (Cluster 6) includes a strengthening of the high pressure ridge towards the continental Baltic area for the extremes composite (Fig. 34), however it has lost importance during the EMULATE period (Fig. 33). Altogether, within-type variations of large-scale circulation types (e.g. Beck et al. 2007) seem to play a major role in the relationships between atmospheric circulation and climate extremes.

Fig. 27: Percentages of days with extreme Central European daily precipitation (beyond the 95th percentile) and without such extremes for the Central European Grosswettertypes (see Fig. 26) during the 2-month winter season January/February.

Jan./Feb.-season, 95th percentile of daily T mean

Fig. 28: Percentages of days with extreme Central European daily mean temperature (beyond the 95th percentile) and without such extremes for the Central European Grosswettertypes (see Fig. 26) during the 2-month winter season January/February.

Jan./Feb.-season, 95th percentile of daily T mean

Fig. 29: Percentages of days with extreme Central European daily mean temperature (beyond the 95th percentile) and without such extremes for the daily MSLP Clusters 1-7 (see EMULATE website) during the 2-month winter season January/February.

53

Fig. 30: Daily MSLP composites for days with extreme Central European daily mean temperature (beyond the 95th percentile) and without such extremes (randomly sampled with the same sample size) for MSLP Cluster 6 (see EMULATE website) of the 2-month winter season (JF) 1901-1951.
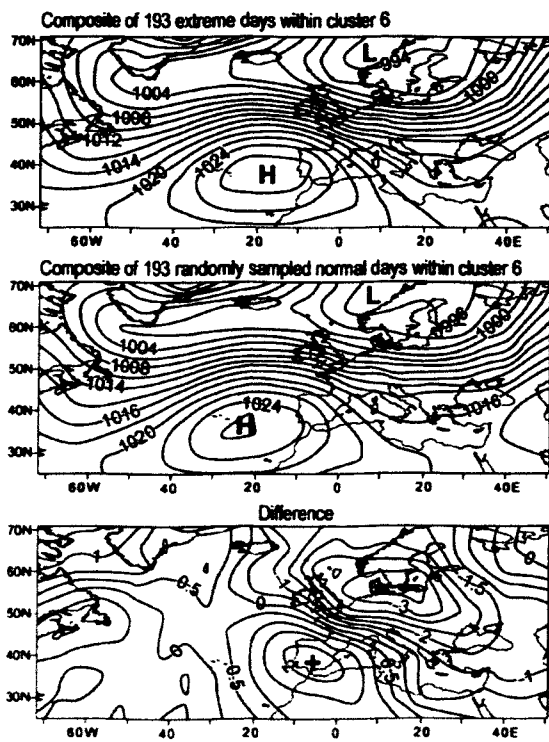
Fig. 31: Daily MSLP composites for days with extreme Central European daily precipitation (beyond the 95th percentile) and without such extremes (randomly sampled with the same sample size) for MSLP Cluster 6 (see EMULATE website) of the 2-month winter season (JF) 1850-2003.
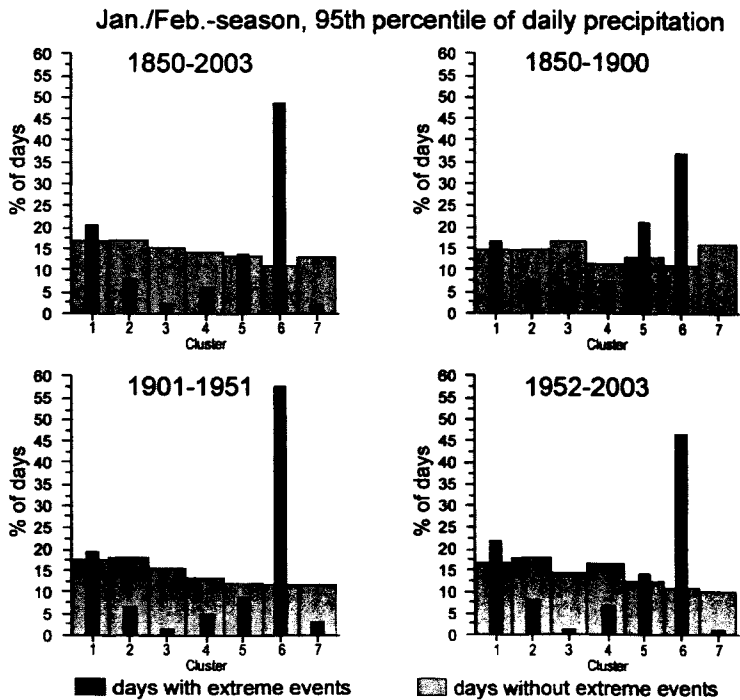
54
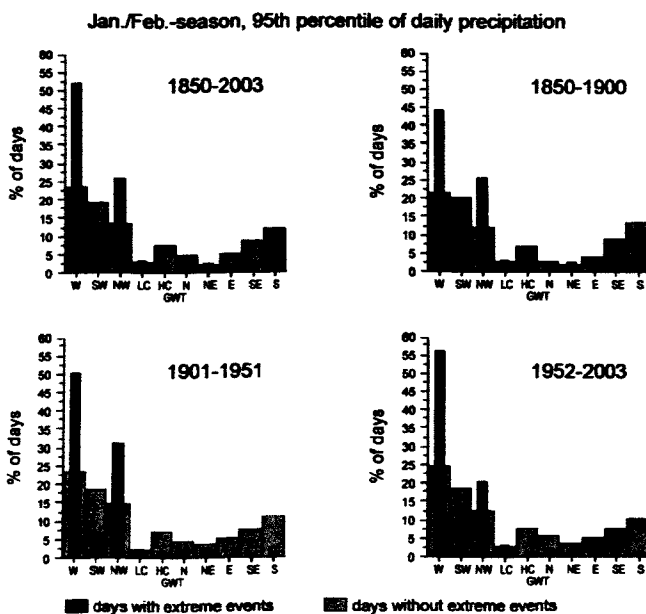
Jan./Feb.-season, 95th percentile of daily precipitation

Fig. 32: Percentages of days with extreme Central European daily precipitation (beyond the 95th percentile) and without such extremes for the daily MSLP Clusters 1-7 (see EMULATE website) during the 2-month winter season January/February.

JJA-season, 95th percentile of daily T mean
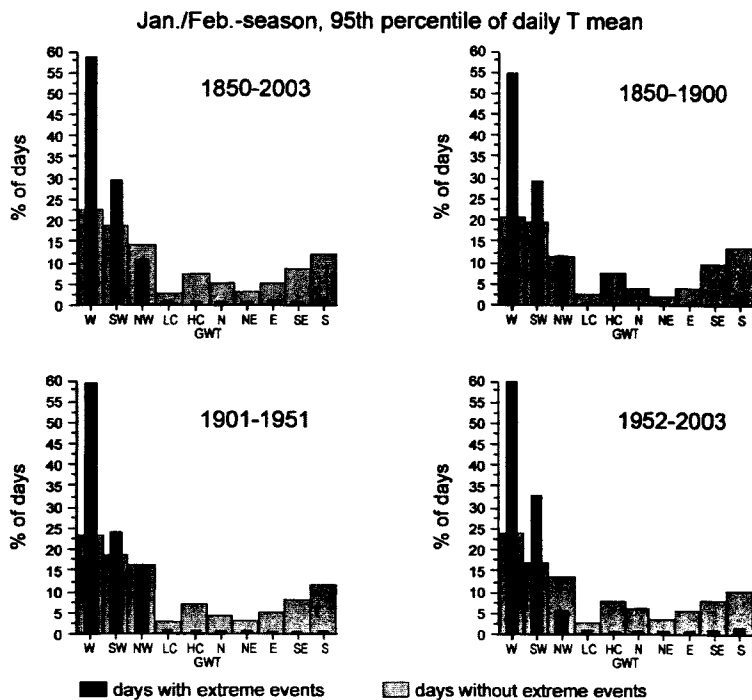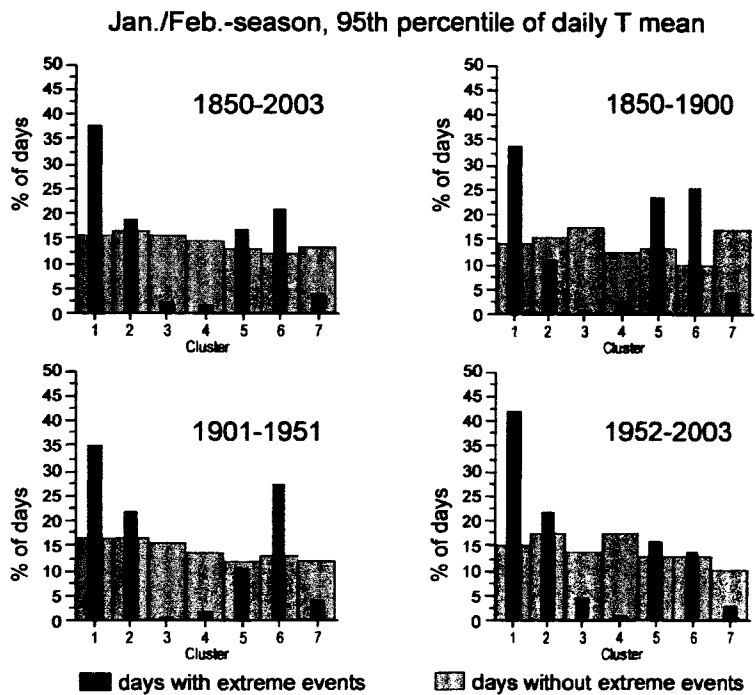

Fig. 33: Percentages of days with extreme Central European daily mean temperature (beyond the 95th percentile) and without such extremes for the daily MSLP Clusters 1-6 (see EMULATE website) during the 3-month summer season JJA.

Composite of 140 extreme days within cluster 6

Composite of 140 randomly sampled normal days within cluster 6
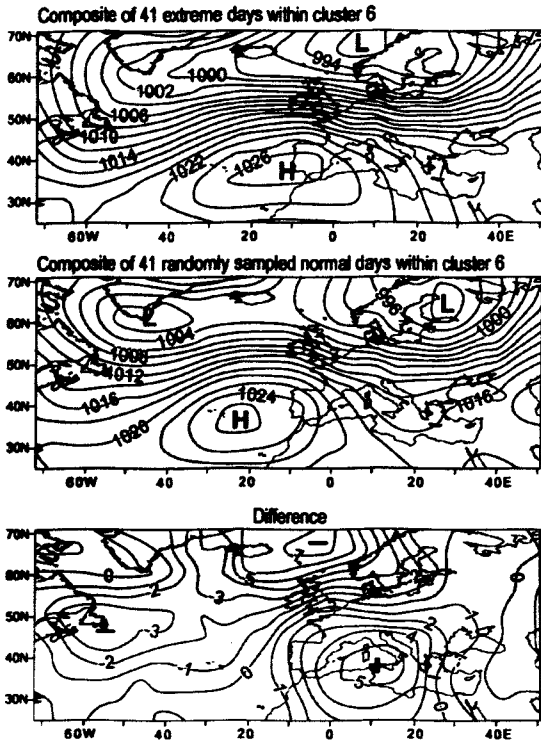
Difference

Fig. 34: Daily MSLP composites for days with extreme Central European daily mean temperature (beyond the 95th percentile) and without such extremes (randomly sampled with the same sample size) for MSLP Cluster 6 (see EMULATE website) of the summer season (JJA) 1850-2003.
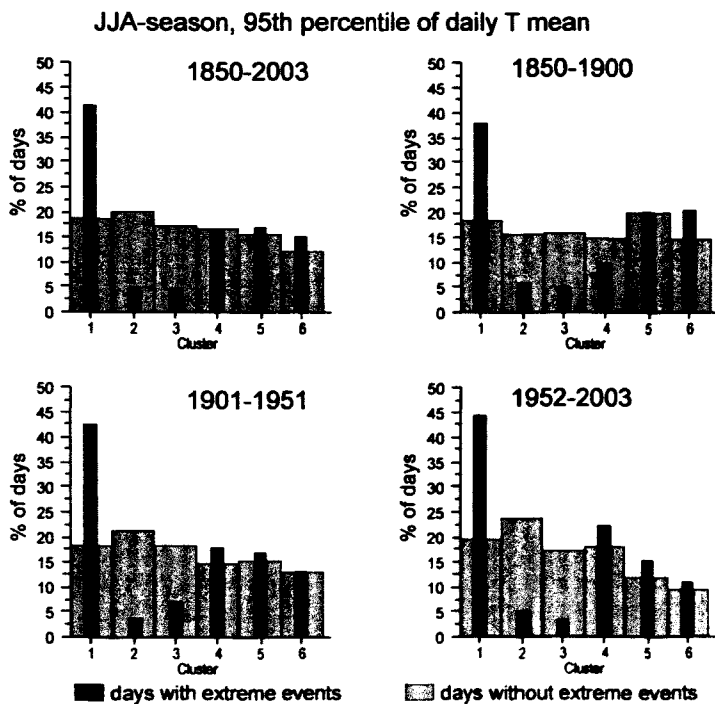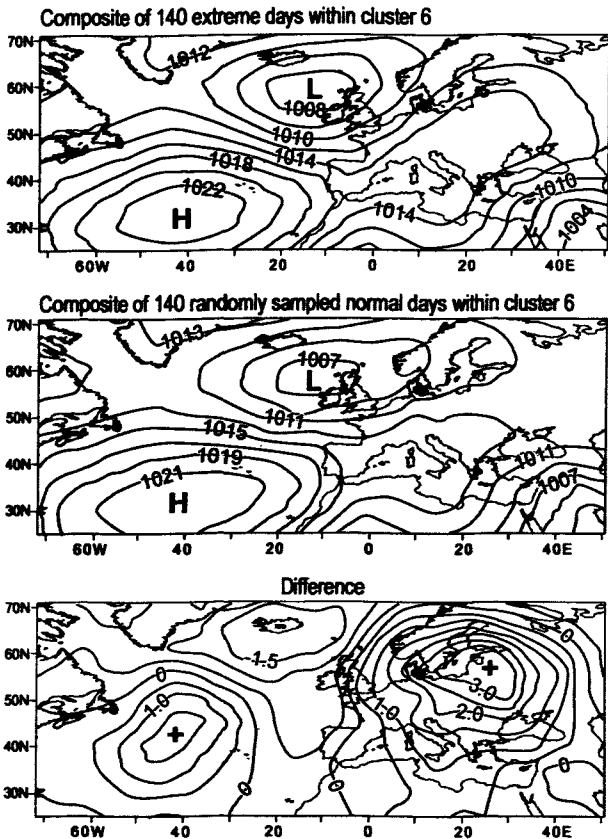
6.2 PCA-derived circulation patterns in relation to temperature and precipitation extremes

Referring to the regional daily temperature and precipitation time series for Germany, all days of the EMULATE period 1850-2003 exceeding the 98th percentile or (for temperature only) falling below the 2nd percentile have been selected separately for each 3-month season. The corresponding daily MSLP fields have been submitted to varimax-rotated T-mode principal component analyses in order to determine the major circulation patterns (>5% of explained variance) occurring during these extreme events. Additional analyses have been performed by including the four preceding days of each extreme event, leading to so-called extended PCAs (cp. Jacobeit et al. 2006) and resulting major sequences of daily circulation patterns related to these extreme events. The complete results are available from the EMULATE website, some few examples will be discussed in the following. Fig. 35 shows the major circulation patterns for heavy Central European precipitation during winter including (as second PC) a northwesterly pattern similar to the Cluster-6 extreme-composite (Fig. 31), a blocking pattern with a strong Atlantic low and a distinct Russian high (PC 1) and a monopole pattern with a southward shifted low above the Atlantic Ocean (PC 3). Fig. 36 reproduces these patterns (with some change in ranking) as extended pattern sequences showing some particular developments in circulation dynamics: for the first PC the gradual transition from a zonal pattern towards a southward extending low in the European sector, for the second PC a weakening and slowly eastward retreating Russian high. The

56

latter sequence is connected with a transition for Central Europe from a RHeast (Russian high with easterly components above Central Europe) to a RHwest pattern (Jacobeit et al. 2003). This means a gradual advance of westerly disturbances towards Central Europe despite the persisting and only slightly eastward shifting large-scale pressure pattern. The third PC sequence depicts a nearly stationary southwest-flow pattern in front of the Atlantic low pressure system.

The second example referring to Central European extremely cold days in winter mainly includes patterns with different blocking highs (Fig. 37): above Russia (corresponding to a RHeast pattern), above Western and Central Europe itself, and around Iceland representing a NAO reversal with northerly components over some parts of Central Europe. Only the fourth PC depicts a relatively weak high pressure influence (eastern Central Europe) being not removed by the strong Atlantic low. As Fig. 38 indicates, all patterns are characterised by a high degree of persistence during the preceding days of these cold extremes. Further work has to be done especially with respect to the above-mentioned within-type variations as a major factor for extremes.
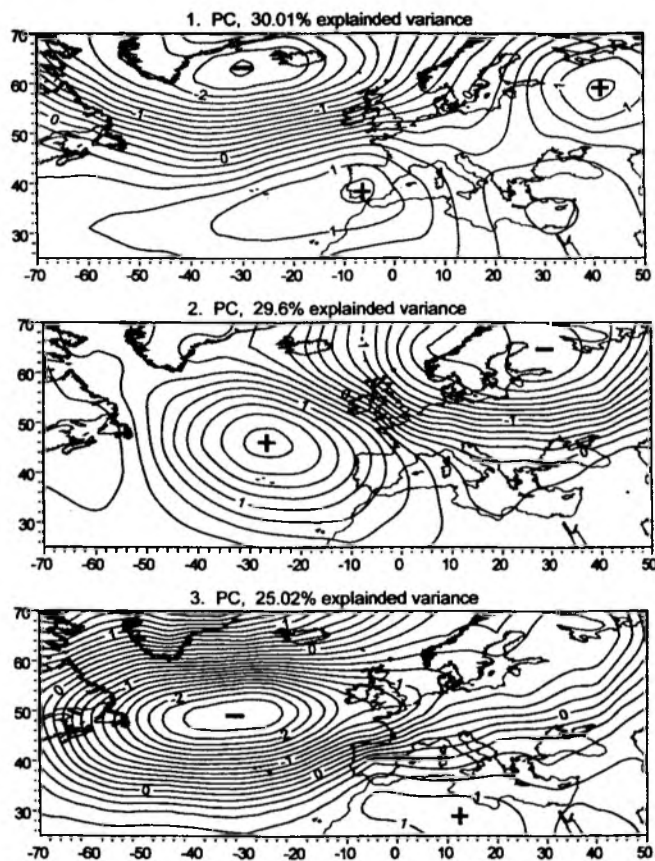
Fig. 35: Normalised circulation patterns of the first 3 T-mode principal components of daily MSLP fields from days with extreme Central European precipitation (beyond the 98th percentile) during the winter season (DJF) 1850-2003.
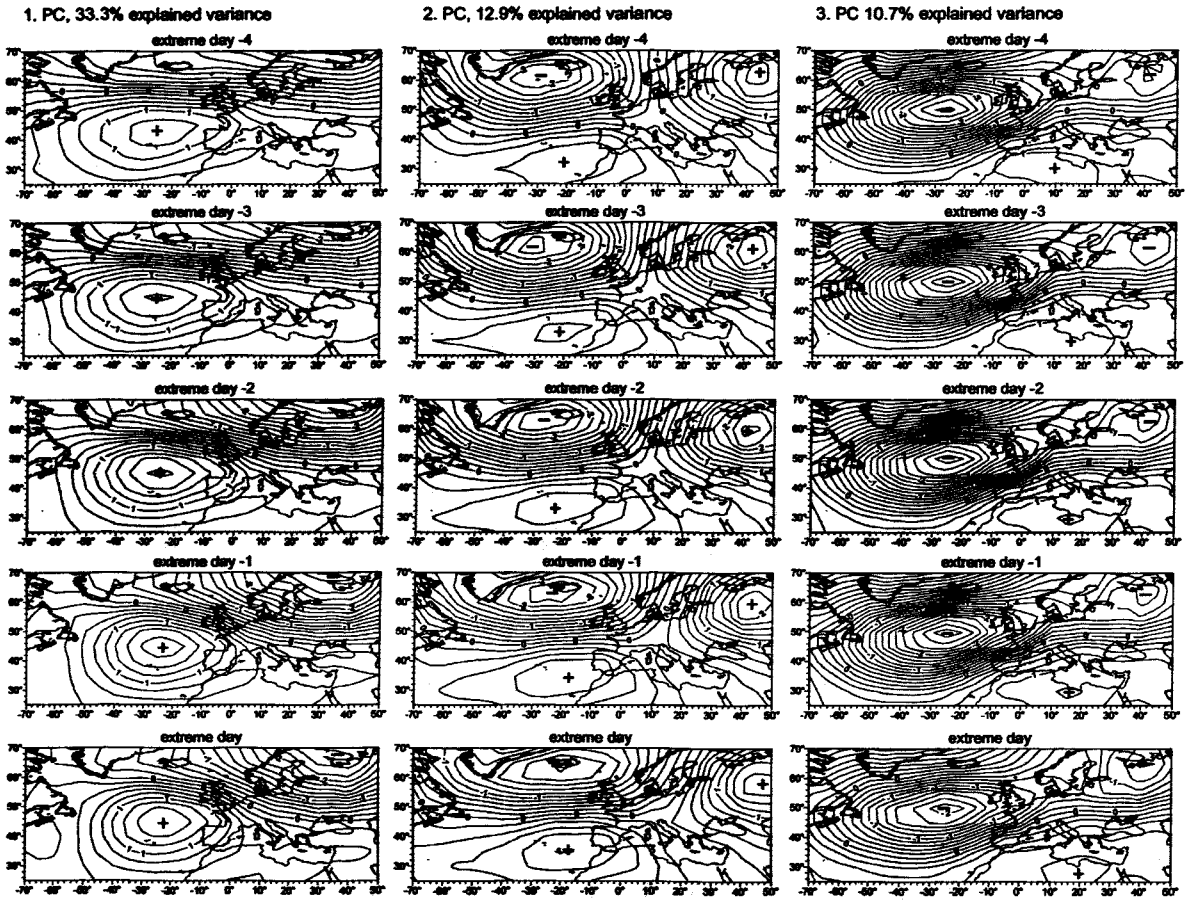
Fig. 36: Normalised circulation pattern sequences from 4 days before an extreme Central European precipitation event (beyond the 98th percentile) resulting as the first 3 modes from an extended T-mode principal component analysis of all corresponding daily MSLP field sequences during the winter season (DJF) 1850-2003.
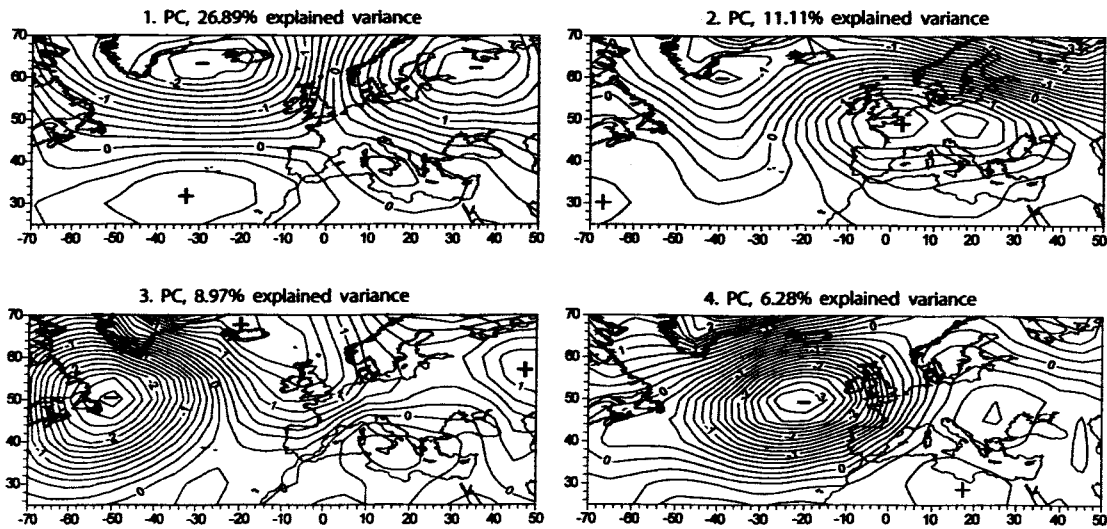
Fig. 37: Normalised circulation patterns of the first 4 T-mode principal components of daily MSLP fields from days with extremely low Central European daily mean temperature (below the 2nd percentile) during the winter season (DJF) 1850-2003.
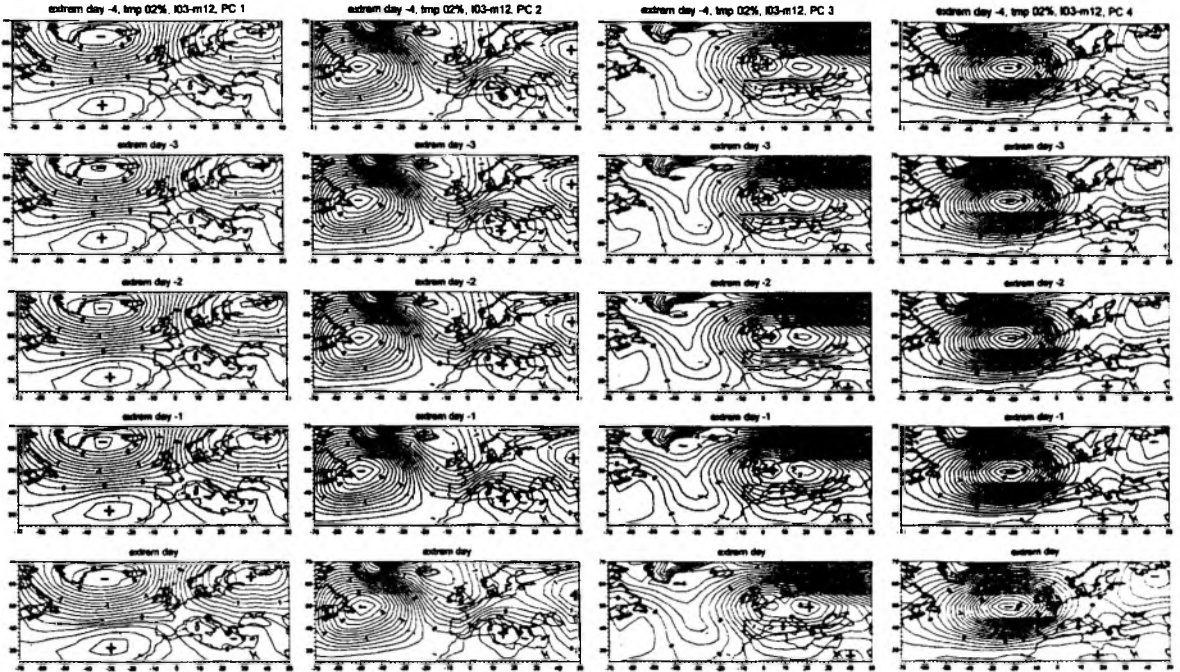
Fig. 38: Normalised circulation pattern sequences from 4 days before an extremely low Central European daily mean temperature (below the 2nd percentile) resulting as the first 4 modes from an extended T-mode principal component analysis of all corresponding daily MSLP field sequences during the winter season (DJF) 1850-2003.

7 Summary of important contributions to EMULATE by the German working group

The European research project EMULATE (European and North Atlantic daily to multidecadal climate variability) was funded by the European Commission from November 2002 until February 2006 and has been co-ordinated by Prof. Phil Jones from the Climatic Research Unit (CRU) at the University of East Anglia (Norwich, UK).

A major focus of EMULATE has been on studies to define extreme climate events based on long daily temperature and precipitation time series across Europe and to determine atmospheric circulation patterns which favour the occurrence of these extreme events. Therefore, EMULATE has provided more than 150 years of gridded daily mean sea-level pressure (MSLP) data for the extratropical North Atlantic and European region (25°N to 70°N, 70°W to 50°E with a 5° by 5° grid resolution). These data have been used by the German working group and associated project partners to develop daily and longer time-scale characteristic atmospheric circulation patterns over the study region for each overlapping two-month season (JF, FM, MA, AM, MJ, JJ, JA, AS, SO, ON, ND, DJ) and each traditional three-month season (DJF, MAM, JJA, SON)[2] of the year.

A wide range of statistical techniques has been applied in order to define leading atmospheric circulation patterns for two-month and three-month seasons, including S-mode and T-mode principal component analyses, k-means cluster analysis, an optimizing cluster algorithm with several randomizations, the simulated annealing clustering technique, and a novel approach merging the last two concepts called SANDRA (simulated annealing and diversified randomization, see Philipp et al. 2007). This novel approach was able to avoid local optima reached by chance and ensured a very close approximation of the global optimum in all cases for the different seasons (Philipp et al. 2007). Therefore it was chosen as the most appropriate technique for defining leading atmospheric circulation patterns for EMULATE. Furthermore, this highly sophisticated classification has become part of the COST Action 733 dealing with Harmonisation and Applications of Weather Type Classifications for European Regions (Jacobeit 2009, Philipp et al. 2010). Thus, it represents significant progress in both methodological development as well as research applications.

One important example of leading atmospheric circulation patterns referring to high winter conditions (January/February) includes two more or less zonal patterns (MSLP Clusters 1 and 6) which are, however, predominantly linked with different meteorological extremes over Central Europe: Cluster 1 resembling the positive mode of the NAO, covers most of the extremely warm winter days, whereas Cluster 6 with its southeastward shifted low pressure centre is most important for extreme precipitation during this season. Thus, the daily MSLP classification achieved by the SANDRA technique proved to be highly consistent with particular differences in circulation dynamics known from synoptic climatology.

Time coefficients of the cluster patterns based on (non-inverted) Euclidean distances were used as pattern amplitudes (increasing values for growing dissimilarities with the corresponding cluster centroids), and their extremes were defined in terms of particular percentiles (2nd, 5th, 10th, 90th, 95th, 98th). Concerning the amplitude extremes only few significant trends can be observed.

In order to characterize within-pattern variability, several parameters have been calculated on a daily basis: a correlation-based approximation for the relative vorticity within the area 40-60°N, 10°W-30°E; an intensity index measuring the pressure gradients between the corresponding

---

[2] JF: January, February – FM: February, March - ... - DJF: December, January, February - ...

centres of action; cluster-related temperature and precipitation indices based on 14 and 25 Central European stations, respectively. All these indices have been calculated as normalized 31-year moving averages for all the seasonal cluster patterns. One important example, concerning within-pattern vorticity and precipitation, is related to the NAO-like cluster 1 for winter which reveals increases to higher levels since the 1920s, but with subsequently larger amplitudes for vorticity than for precipitation.

In order to achieve a closer correspondence of circulation patterns to regional extremes in temperature and precipitation, an objective classification into Central European Grosswettertypes (GWT, see Beck et al. 2007) has been adopted to the daily scale (in addition to the above-mentioned SANDRA classification). These patterns include ten major types according to the main flow directions (W, SW, ...) and to regional pressure centres (High above Central Europe; Low above Central Europe), likewise used for studies on circulation-climate relationships.

Additionally, a new database containing European station data for temperature and precipitation with a daily resolution has been generated, further extending earlier data sets. This database has been used for calculating 64 different extremes indices allowing to relate variations and trends in atmospheric circulation patterns to prominent extremes in temperature and precipitation.

For each season and for each of the percentile-based extreme types, frequency distributions of days with and without a particular extreme in dependence of the circulation types (cluster patterns as well as GWTs) have been calculated for the whole EMULATE period 1850-2003 and for three ~50-year subperiods. In most cases only some few of the circulation types proved to be conducive to extreme events, for example – with respect to heavy Central European precipitation during high winter (JF) – a pattern with southeastward shifted low pressure influence from subpolar latitudes towards the European continent (see also Jacobeit et al. (2009) with respect to the 3-month season DJF). MSLP composite analyses for days with extreme and non-extreme daily temperature and precipitation additionally indicate important within-type variations as for example the tendency towards zonal circulation patterns for Central European warm extremes during winter in contrast to southeastward shifted subpolar low pressure for precipitation extremes (see also Jacobeit et al. 2009).

Finally, daily MSLP fields selected for particular extremes in Central Europe have also been submitted to T-mode principal component analyses (both in ordinary way and extended to principal sequence pattern analyses) confirming circulation-climate relationships indicated by the above-mentioned classification approaches. In conclusion, synoptic approaches of downscaling with respect to temperature and precipitation extremes seem to be promising and will further be developed in forthcoming projects.

References

Bahrenberg, G., E. Giese, & J. Nipper (1999): Statistische Methoden in der Geographie 1. - Teubner, Stuttgart, Germany, pp. 233.

Beck, C. (2000): Zirkulationsdynamische Variabilität im Bereich Nordatlantik-Europa seit 1780. – Würzburger Geographische Arbeiten 95, Würzburg, 350S.

Beck, C., J. Jacobeit & P.D. Jones (2007): Frequency and within-type variations of large-scale circulation types and their effects on low-frequency climatic variability in Central Europe since 1780. - Int. J. Climatol. 27: 473-491.

Beck, C., A. Philipp & J. Jacobeit (2007): An intercomparison of selected circulation type classifications for the European region. - Geophysical Research Abstracts, Vol. 9, 10659, 2007.

Bhend, J. (2005): North Atlantic and European Cyclones: Their Variability and Change from 1881 to 2003. - Master Thesis. Institute of Geography, University of Bern, Switzerland.

Chen, D., A. Walther, A. Moberg, P. Jones, J. Jacobeit & D. Lister (2007): Trends of extreme temperature and precipitation climates in Europe: A trend atlas of the EMULATE indices. - Gothenburg 2007, 794 pp.

Della-Marta, P.M. & H. Wanner (2006): A Method of Homogenizing the Extremes and Mean of Daily Temperature Measurements. - J. Climate 19: 4179-4197.

Hertig, E. & J. Jacobeit (2008): Assessments of Mediterranean precipitation changes for the 21st century using statistical downscaling techniques. - Int. J. Climatol. DOI 10.1002/joc.1597.

Hertig, E. & J. Jacobeit (2008): Downscaling Future Climate Change: Temperature Scenarios for the Mediterranean area. - Special Issue of Global and Planetary Change: 127-131.

Jacobeit, J., C. Beck & A. Philipp (1998): Annual to Decadal Variability in Climate in Europe – Objectives and Results of the German Contribution to the European Climate Research Project ADVICE. – Würzburger Geographische Manuskripte 43, 163 pp.

Jacobeit, J. & A. Dünkeloh (2005): The Eastern Mediterranean Transient in Relation to Atmospheric Circulation Dynamics. - Hydrogeologie und Umwelt, 33(5), 2005, 1-8.

Jacobeit, J., P. Jones, T. Davies & C. Beck (2001): Circulation changes in Europe since the 1780s. - In: History and Climate: Memories of the Future? (ed. by P. Jones, A. Ogilvie, T. Davies & K. Briffa), Kluwer Academic/Plenum, 2001, 79-99.

Jacobeit, J., M. Nonnenmacher & A. Philipp (2003): Atmosphärische Zirkulationsdynamik markanter Abflussereignisse in Mitteleuropa. - Terra Nostra, 2003/6, 209-213.

Jacobeit, J. H. Wanner, J. Luterbacher, C. Beck, A. Philipp & K. Sturm (2003): Atmospheric circulation variability in the North-Atlantic-European area since the mid-seventeenth century. - Clim Dyn 20: 341-352.

Jacobeit, J., A. Philipp & M. Nonnenmacher (2006): Atmospheric circulation dynamics linked with prominent discharge events in Central Europe. - Hydrological Sciences Journal, 51(5), 178-197.

Jacobeit, J., J. Rathmann, A. Philipp & P.D. Jones (2009): Central European precipitation and temperature extremes in relation to large-scale atmospheric circulation types. - Met. Zeitschrift 18, 397-410.

Jacobeit, J. (2009): Classifications in Climate Research. - Physics and Chemistry of the Earth (accepted for publication).

Jones, P.D., Horton, E.B., Folland, C.K., Hulme, M., Parker, D.E., Basnett, T.A. (1999): The use of indices to identify changes in climatic extremes. - Climatic Change 42: 131-149.

Luterbacher, J., Xoplaki, E., Dietrich, D., Rickli, R., Jacobeit, J., Beck, C., Gyalistras, D., Schmutz, C., Wanner, H. (2002): Reconstruction of Sea Level Pressure fields over the Eastern North Atlantic and Europe back to 1500. - Clim. Dyn. 18: 545-561.

Luterbacher, J., E. Xoplaki, C. Casty, H. Wanner, A. Pauling, M. Kuettel, T. Rutishauser, S. Broennimann, E. Fischer, D. Fleitmann, J.F. Gonzalez-Rouco, R. Garcia-Herrera, M. Barriendos, F.S. Rodrigo, J.C. Gonzalez-Hidalgo, M.A. Saz, L. Gimeno, P. Ribera, M. Brunet, H. Paeth, N. Rimbu, T. Felis, J. Jacobeit, A. Duenkeloh, E. Zorita, J. Guiot, M. Turkes, M.J. Alcoforado, R. Trigo, D. Wheeler, SFB. Tett, M.E. Mann, R. Touchan, D.T. Shindell, S. Silenzi, P. Montagna, D. Camuffo, A. Mariotti, T. Nanni, M. Brunetti, M. Maugeri, C. Zerefos, S. De Zolt, P. Lionello, M.F. Nunes, V. Rath, H. Beltrami, E. Garnier & E. Le Roy Ladurie (2006): Mediterranean climate variability over the last centuries: A review. - In: Lionello, P., Malanotte-Rizzoli, P., & Boscolo, R [Eds.] (2006): The Mediterranean Climate: an overview of the main characteristics and issues. - Elsevier, Amsterdam, 27-148.

Moberg, A., P.D. Jones, D. Lister, A. Walther, M. Brunet, J. Jacobeit, L.V. Alexander, P. Della-Marta, J. Luterbacher, P. Yiou, D. Chen, A. Klein Tank, O. Saladié, J. Sigró, E. Aguilar, H. Alexandersson, C. Almarza, I. Auer, M. Barriendos, M. Begert, H. Bergström, R. Böhm, C. J. Butler, J. Caesar, A. Drebs, D. Founda, F.-W. Gerstengarbe, G. Micela, M. Maugeri, H. Österle, K. Pandzic, M. Petrakis, L. Srnec, R. Tolasz, H. Tuomenvirta, P.C. Werner, H. Linderholm, A. Philipp, H. Wanner & E. Xoplaki (2006): Indices for daily temperature and precipitation extremes in Europe analysed for the period 1901-2000. – In: J. Geophys. Res. - Atmospheres, 111, D22106, 2006, doi: 10.1029/2006JD007103

Murray, R. & Simmonds, I. (1991): A numerical scheme for tracking cyclone centres from digital data, Part I: development and operation of the scheme. - Australian Meteorological Magazine, 39, 155-166.

Philipp, A. & J. Jacobeit (2003): Das Hochwasserereignis in Mitteleuropa im August 2002 aus klimatologischer Perspektive. - Petermanns Geographische Mitteilungen, 147, 2003/6, 50-52.

Philipp, A., J. Jacobeit, P. Della-Marta & D. Fereday (2005): Classification of reconstructed daily pressure patterns for the period 1850 to 2003 in the North-Atlantic-European Region. – Geophysical Research Abstracts, Vol. 7, 08837, 2005.

Philipp, A., P.M. Della-Marta, J. Jacobeit, D.R. Fereday, P.D. Jones, A. Moberg & H. Wanner (2007): Long term variability of daily North Atlantic–European pressure patterns since 1850 classified by simulated annealing clustering. – J. Climate 20: 4065–4095.

Philipp A., J. Bartholy, C. Beck, M. Erpicum, P. Esteban, X. Fettweis, R. Huth, P. James, S. Jourdain, F. Kreienkamp, T. Krennert, S. Lykoudis, S. Michalides, K. Pianko, P. Post, D. Rasilla

Álvarez, R. Schiemann, A. Spekat, F. S. Tymvios (2010): COST733CAT - a database of weather and circulation type classifications. Physics and Chemistry of the Earth, submitted.

Rathmann, J., A. Philipp & J. Jacobeit (2006): Classification of reconstructed daily SLP patterns 1850-2003 and links to the occurrence of extreme events in Central European climate. - Geophys. Res. Abstr. Vol. 8, No EGU06-A-08737.

Trigo, R., E. Xoplaki, E. Zorita, J. Luterbacher, S.O. Krichak, P. Alpert, J. Jacobeit, J. Sáenz, J. Fernández, F. González-Rouco, R. Garcia-Herrera, X. Rodo, M. Brunetti, T. Nanni, M. Maugeri, M. Türkes, L. Gimeno, P. Ribera, M. Brunet, I.F. Trigo, M. Crepon & A. Mariotti (2006): Relations Between Variability in the Mediterranean Region and Mid-Latitude Variability. - In: Lionello, P., Malanotte-Rizzoli, P., & Boscolo, R. [Eds.] (2006): The Mediterranean Climate: an overview of the main characteristics and issues. - Elsevier, Amsterdam, 173-216.

Walther, A. (2004): The development in time and the spatial distribution of precipitation- and temperature-extremes over Europe since 1850. - Diploma Thesis, Univ. of Würzburg, 2004.

Zhang, X., G. Hegerl, F.W. Zwiers & J. Kenyon (2004): Avoiding inhomogeneity in percentile-based indices of temperature extremes. - J. Climate 18: 1641-1651.

Websites:

ECA: European Climate Assessment (http://eca.knmi.nl)
EMULATE: EU project Emulate (http://www.cru.uea.ac.uk/projects/emulate)
EMULATE: German contributions to EMULATE (http://geo21/emulate)
STARDEX: EU project Stardex (http://www.cru.uea.ac.uk/projects/stardex)

GEOGRAPHICA AUGUSTANA

EMULATE

The European climate research project EMULATE (European and North Atlantic daily to MULtide-cadal climATE variability), funded by the European Commission, has created daily gridded fields of mean sea-level pressure (MSLP) over the extratropical North Atlantic and Europe (25°N to 70°N; 70°W to 50°E on a 5° by 5° grid spacing), 1850 to date.

A wide range of statistical techniques has been applied in order to define leading atmospheric circulation patterns for two-month and three-month seasons, including S-mode and T-mode principal component analyses, k-means cluster analysis, an optimizing cluster algorithm with several randomizations, the simulated annealing clustering technique, and a novel approach merging the last two concepts called SANDRA (simulated annealing and diversified randomi-zation).

A major focus of EMULATE has been on studies to define extreme climate events based on long daily temperature and precipitation time series across Europe and to determine atmospheric circulation patterns which favour the occurrence of these extreme events.

Variations in the incidence of extremes of temperature and precipitation (including drought) across Europe have been related to fluctuations and trends in the atmospheric circulation pat-terns on daily to multi-decadal time-scales.